ADVANCED CURRENT COLLECTION RESEARCH

Annual Technical Report

for Period Ending 28 February 1977

Submitted to

Advanced Research Projects Agency

C. J. Mole, D. L. Greene, I. R. McNab,
J. L. Johnson, O. S. Taylor, W. R. Gass,
and P. K. Lee

D D C

APR 5 1978
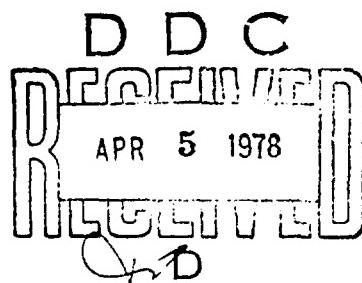
Approved:

J. K. Hulm, Manager
Chemical Sciences Division

Westinghouse R&D Center
1310 Beulah Road
Pittsburgh, Pennsylvania 15235

DOCUMENT CONTROL DATA - R&D

(Security classification of title, body of abstract and indexing annotation must be entered when the overall report is classified)

1. ORIGINATING ACTIVITY (Corporate author)	2a. REPORT SECURITY CLASSIFICATION
Westinghouse Electric Corporation Research Laboratories Churchill, PA 15235	Unclassified
	2b. GROUP

3. REPORT TITLE

ADVANCED CURRENT COLLECTION RESEARCH

4. DESCRIPTIVE NOTES *(Type of report and inclusive dates)*

Annual Technical Report - for period ending 28 February 1977.

5. AUTHOR(S) *(Last name, first name, initial)*

Mole, C.J.; Greene, D.L.; Johnson, J.L.; McNab, I.R.; Taylor, O.D.; Lee, P.K.; and Gass, W.R.

6. REPORT DATE	7a. TOTAL NO. OF PAGES	7b. NO OF REFS
May 1977	90	0

8a. CONTRACT OR GRANT NO.	9a. ORIGINATOR'S REPORT NUMBER(S)
N00014-76-C-0683	77-8B20-AMCOL-R1
b. PROJECT NO.	
c.	9b. OTHER REPORT NO(S) (Any other numbers that may be assigned this report)
d.	

DISTRIBUTION STATEMENT A

Approved for public release;
Distribution Unlimited

11. SUPPLEMENTARY NOTES	12. SPONSORING MILITARY ACTIVITY
	Advanced Research Projects Agency Dept. of Defense, 1400 Wilson Blvd. Arlington, VA 22209

13. ABSTRACT

This program is for the research and development of advanced, solid-brush current collection systems for application to innovative electrical machinery. The objectives of the program are to increase the useful lifetime, reduce the sliding contact losses and increase the operating current density of solid brushes operating to transfer current between moving portions of electrical machines. The advances in current collector performance can be utilized to satisfy the requirements for electrical machines of high power density.

The report covers the first year of work, during which time a spectrum of brush and slip ring materials were characterized and promising candidate materials selected for in-depth testing. Two, high-speed test rigs were commissioned to extend the brush performance range to anticipated machine speeds. The fundamental aspects of the sliding interface were investigated, and directions of future research established. Fiber brushes were developed and tested to examine the the potential of this promising concept.

DD FORM **1473**
JAN 64

14. KEY WORDS	LINK A		LINK B		LINK C	
	ROLE	WT	ROLE	WT	ROLE	WT
contacts sliding carbon fibers brushes atmosphere shunts loading friction wear graphite slip rings						

INSTRUCTIONS

1. ORIGINATING ACTIVITY: Enter the name and address of the contractor, subcontractor, grantee, Department of Defense activity or other organization *(corporate author)* issuing the report.

2a. REPORT SECURITY CLASSIFICATION: Enter the overall security classification of the report. Indicate whether "Restricted Data" is included. Marking is to be in accordance with appropriate security regulations.

2b. GROUP: Automatic downgrading is specified in DoD Directive 5200.10 and Armed Forces Industrial Manual. Enter the group number. Also, when applicable, show that optional markings have been used for Group 3 and Group 4 as authorized.

3. REPORT TITLE: Enter the complete report title in all capital letters. Titles in all cases should be unclassified. If a meaningful title cannot be selected without classification, show title classification in all capitals in parenthesis immediately following the title.

4. DESCRIPTIVE NOTES: If appropriate, enter the type of report, e.g., interim, progress, summary, annual, or final. Give the inclusive dates when a specific reporting period is covered.

5. AUTHOR(S): Enter the name(s) of author(s) as shown on or in the report. Enter last name, first name, middle initial. If military, show rank and branch of service. The name of the principal author is an absolute minimum requirement.

6. REPORT DATE: Enter the date of the report as day, month, year; or month, year. If more than one date appears on the report, use date of publication.

7a. TOTAL NUMBER OF PAGES: The total page count should follow normal pagination procedures, i.e., enter the number of pages containing information.

7b. NUMBER OF REFERENCES: Enter the total number of references cited in the report.

8a. CONTRACT OR GRANT NUMBER: If appropriate, enter the applicable number of the contract or grant under which the report was written.

8b, 8c, & 8d. PROJECT NUMBER: Enter the appropriate military department identification, such as project number, subproject number, system numbers, task number, etc.

9a. ORIGINATOR'S REPORT NUMBER(S): Enter the official report number by which the document will be identified and controlled by the originating activity. This number must be unique to this report.

9b. OTHER REPORT NUMBER(S): If the report has been assigned any other report numbers *(either by the originator or by the sponsor)*, also enter this number(s).

10. AVAILABILITY/LIMITATION NOTICES: Enter any limitations on further dissemination of the report, other than those imposed by security classification, using standard statements such as:

 (1) "Qualified requesters may obtain copies of this report from DDC."

 (2) "Foreign announcement and dissemination of this report by DDC is not authorized."

 (3) "U. S. Government agencies may obtain copies of this report directly from DDC. Other qualified DDC users shall request through

 _____ ."

 (4) "U. S. military agencies may obtain copies of this report directly from DDC. Other qualified users shall request through

 _____ ."

 (5) "All distribution of this report is controlled. Qualified DDC users shall request through

 _____ ."

 If the report has been furnished to the Office of Technical Services, Department of Commerce, for sale to the public, indicate this fact and enter the price, if known.

11. SUPPLEMENTARY NOTES: Use for additional explanatory notes.

12. SPONSORING MILITARY ACTIVITY: Enter the name of the departmental project office or laboratory sponsoring *(paying for)* the research and development. Include address.

13. ABSTRACT: Enter an abstract giving a brief and factual summary of the document indicative of the report, even though it may also appear elsewhere in the body of the technical report. If additional space is required, a continuation sheet shall be attached.

 It is highly desirable that the abstract of classified reports be unclassified. Each paragraph of the abstract shall end with an indication of the military security classification of the information in the paragraph, represented as *(TS)*, *(S)*, *(C)*, or *(U)*.

 There is no limitation on the length of the abstract. However, the suggested length is from 150 to 225 words.

14. KEY WORDS: Key words are technically meaningful terms or short phrases that characterize a report and may be used as index entries for cataloging the report. Key words must be selected so that no security classification is required. Identifiers, such as equipment model designation, trade name, military project code name, geographic location, may be used as key words but will be followed by an indication of technical context. The assignment of links, rules, and weights is optional.

PROPRIETARY RESTRICTIONS

The material identified below should be treated as proprietary
to protect certain patent rights until U.S. patent applications are filed
or for a time not to exceed six (6) months from date of this report.

Proprietary Material

Section 1.3.3, Page 1-5.

Section 4, Pages 4-1 through 4-14.

Does not apply
3/16/78
ONR
Code 473

ADVANCED CURRENT COLLECTION RESEARCH

Annual Technical Report for the Period
Ending 28 February 1977

Sponsored by Advanced Research Projects
Agency, Department of Defense

Contract N00014-76-C-0683

Research Report 77-8820-AMCOL-R1

May 1977

WESTINGHOUSE ELECTRIC CORPORATION   PITTSBURGH, PA 15235

TABLE OF CONTENTS

LIST OF FIGURES

LIST OF TABLES

SECTION 1

INTRODUCTION AND SUMMARY

1.0 BACKGROUND

As a result of promising research efforts conducted by
Westinghouse Electric Corporation in the area of high performance solid
brush current collection systems, the final phase of ARPA Contract
DAHC 15-72-C-0229, Design and Development of a Segmented Magnet Homopolar
Torque Converter, incorporated an initial series of screening tests to
identify the degree of promise attending the search for a high current
density, long-lived solid brush. The initial results were sufficient to
warrant the establishment of a broadly based program, and the following
report documents the first year of effort in that program. The high
degree of interest in a high performance solid brush follows from increasing
needs, in various DOD sectors, for drive and power machines of high
power density. For electrical machine designs requiring current transfer
from a rotating member to a stationary member, a high current density
collector can substantially reduce overall machine weight and volume.

1.1 OBJECTIVES

The principal objective of the program is to develop solid
brush current collectors with the following capabilities:

- high current density
- low power loss
- high speed
- reversing capability
- long life and high reliability

The general nature of this objective is such that specific goals have been established to measure program progress. The goals were formulated to support ongoing, near-term machine development efforts and long range, more speculative applications. For the near term, the machine operating parameters include:

- current density to 233 A/cm^2
- power loss of 50 watts/cm^2 or less
- sliding speeds up to 4500 meters per minute
- wear rates of 2000 hrs/cm or longer

In setting long range goals, specific values for contact parameters were established resulting in the following set:

- current density to 310 A/cm^2
- double-contact voltage drop of 0.10 V
- sliding speeds up to 4500 meters per minute
- wear rates of 7800 h s/cm

These goals define the initial program motivation, and within their framework the specific planning objectives which were set include:

(a) evaluation of existing solid brush and ring materials and current collection systems to identify development channels.

(b) extension of existing material and fabrication technologies to improve solid brush performance.

(c) development and test of innovative materials, structures and processes to achieve dramatic performance improvements.

The direction for innovative technological solutions to brush interface problems is the outgrowth of initial screening evaluations, extensive review of the state-of-the-art for current collection and tribology, and the creative talent of experts in the current collection field.

1.2 PRIOR AND RELATED WORK

Westinghouse has been investigating the problems of power transfer across sliding electrical contacts (solid brushes) for many years. One of the results of this research was the demonstration that brush life can be increased 10 to 15 times by operating brushes in a humidified, inert gas atmosphere, rather than in air. These brushes are presently operated at a practical application level of 9 A/cm^2.

Previous experimental work at Westinghouse has shown that very high current densities (300 A/cm^2) can be achieved when solid brushes are operating in controlled inert gas atmospheres with water vapor and/or other additives. Furthermore, greatly reduced friction coefficients and voltage drops across the interface have been achieved simultaneously, resulting in a predicted brush life in excess of 8000 hrs/cm.

The initial Westinghouse research work was continued and expanded under an ARPA-sponsored program, titled "Design and Development of a Segmented Magnet Homopolar Torque Converter", Contract No. DAHC 15-72-C-0229. In Phase III-A of that contract, Westinghouse operated a set of laboratory brush testers in a preliminary screening test series to validate previously obtained performance. Additionally, construction of a major, high speed test rig was undertaken. The work which followed in the present program builds on this initial ARPA sponsorship.

The improved operating performance of new brush systems based on this effort will improve the performance of existing commercially available machines, and will improve the applicability and maintainability of advanced concept machines, such as SEGMAG. The realization of this improved performance in practical systems is the central feature of this program.

1.3 SUMMARY OF CURRENT PROGRESS

1.3.1 Current Collector Test Rigs

The conduct of the test program has required tne use of five conventional test rigs and two sophisticated test rigs specifically designed for the program. These include four laboratory rigs for the initial screening of materials and environments, one laboratory rig for the testing of fiber brushes and two high speed, cooled rotor rigs for the close simulation of developmental machine performance.

1.3.1.1 Laboratory Brush Testers

Four laboratory testers were employed in screening a wide range of brush materials, environments and ring materials to identify promising operational candidate materials and development directions. A fifth laboratory tester was modified to accept gas cooled fiber brushes.

1.3.1.2 Machine Environment Brush Tester (MEB)

The MEB was commissioned and operated in an initial test series to characterize the machine. In order to give the test rig a higher speed capability, the soft copper drum was replaced with a CUPALOY drum. The rig was recommissioned and operated in tests.

1.3.1.3 Advanced Brush System Tester (ABS)

A second, cooled-rotor test rig, the ABS, was constructed and tests begun. The rig has several features intended to simulate machine operation, including high speed, a slotted rotor and adequate space to test brush actuation and loading systems.

1.3.2 Current Collector Contact Material Performance

Brush material screening tests resulted in the selection of four candidate materials for continued testing at high speed on the cooled rotor test rigs, including three silver-graphite and one copper graphite grades. Tests of various ring materials indicate that copper and silver based alloys result in the lowest net power loss and longest life for brush operation.

1.3.3 Current Collector Loading Systems

The development of a multi-fiber shunt has continued through two iterations in preparation for dynamic tests against an operating brush. Static tests correlate well with a mathematical description of the voltage drop.

No work was scheduled or undertaken in brush actuation during this period.

1.3.4 Current Collector Gaseous Environment

Five non-oxidizing gases, combined with water vapor, were tested as the atmosphere for the operation of a copper graphite brush on a copper slipring. Similarly, a series of tests employing atmospheres of CO_2 with hydrocarbon vapor addition was run to examine the impact of various vapors on the lubricating properties of graphite. Brush performance was found to be dependent on the selection of the non-oxidizing gas as well as on hydrocarbon molecular weight and vapor concentration.

1.3.5 Fiber Brush Research

Principal efforts have been conducted in the areas of carbon fiber metallization and fiber brush construction. A fiber brush test rig was commissioned and testing undertaken. Tests to date have been accomplished with various atmospheres, but with no forced cooling. Planned tests include gas cooling to permit increased current density operation.

1.3.6 Fundamental Research Projects

The fundamental research projects were divided into three areas: a general state of the art review, development of contact phenomena information, and the establishment of technologically promising approaches for the future of the program.

1.3.6.1 Literature Review

In order to base the material research and development efforts on the most up-to-date information, a literature review was conducted in the relevant areas of the chemical and physico-chemical properties of lamellar solids (mainly graphite and various dichalcogenides) and their interactions with metal surfaces.

1.3.6.2 Contact Phenomena

The impact of hydrocarbon vapors or water vapor present in the atmosphere of graphite and metal-graphite contact systems was measured experimentally. Resistance values as a function of contact force were determined, and a power-law relationship was established.

1.3.6.3 New Concepts for Development

Based on the results of screening tests, contact phenomena experiments, atmosphere variation tests and the literature review, the directions for new material developments were identified, with the objective of reaching the program goals in the most effective manner. Avenues to be pursued include both new materials and new structures for brushes, as well as advanced cooling, shunting and loading techniques.

SECTION 2

CURRENT COLLECTOR TEST RIGS

2.1 OBJECTIVES

The objective of this task was to provide suitable test facilities to support the development of high current brushes for advanced machines. The test rigs were used initially to screen candidate brushes and brush systems, prior to more advanced testing of selected systems on the higher speed, high current density, multiple brush testers which were developed during this reporting period.

2.2 PRIOR AND RELATED WORK

Four existing laboratory "bell-jar" type testers, available from other Westinghouse-funded programs, were modified for use in this program. Descriptions of these testers (B1, B2, HS1, HS2) and their capabilities have been given previously. During this period these have been in continuous operation, providing screening test data on brush and ring materials. A more advanced test rig, the Machine Environment Brush Tester (MEB), was assembled ready for operation. This rig was designed to enable brush and slipring systems to be tested in an environment which closely simulates that of the electromechanical machines, including high currents, multiple (96) brushes, and low-level ambient magnetic fields. A detailed description of this test rig was given previously. Figure 2.1 shows the MEB tester fully assembled.

2.3 CURRENT PROGRESS

2.3.1 Laboratory Brush Testers (B, HS)

The laboratory "bell-jar" type testers were employed during this period to continue the screening of brush and slipring materials and to initiate screening tests of gases and vapor additive materials. The results of this work are described in Sections 3 and 5.

A fifth laboratory "bell-jar" tester was modified and placed in operation for the testing of fiber type brushes. The results of this effort are discussed in Section 6.

2.3.2 Machine Environment Brush Tester (MEB)

The initial assembly of the Machine Environment Brush Tester was completed during this period. Preliminary shake-down runs allowed the electrical design to be verified. Bearing-seal friction and CO_2 windage loss determinations were made throughout the speed range. Because of the need to obtain higher speed brush data than the original construction of the MEB permitted, a new, hard copper (CUPALOY) rotor drum was installed. The tester has now been restored to full service, with a 51 meter-per-second sliding speed capability. Selected materials are being tested at this higher speed.

2.3.3 Advanced Brush System Tester (ABS)

An Advanced Brush System test rig was designed, fabricated, assembled, and commissioned. The purpose of this tester is to evaluate high current brushes and brush systems, including shunts, brush supports, and mechanical loading techniques. In addition to fast turn-around time between tests, the main feature of the ABS tester are summarized in Table 2.1

TABLE 2.1: ABS TESTER

OPERATING CONDITIONS	RESPONSES

- Speed - to 71 m/s
- Current - to 2000 A ($388 A/cm^2$)
- Brushes - 4/track (1 track initially 4 track provision)
- Forced Cooling - collector rotor, brush holders.
- Environment - humidified test gases.

- Brush Contact Voltage
- Brush/ring Friction Drag
- Brush Life
- Current Sharing

A schematic diagram of the ABS test rig is shown in Fig. 2.2 and a photograph of the assembled rig, with the hermetically sealing access cover rolled back, is shown in Fig. 2.3. A portion of the drive system, the torque sensor, current conductor/water cooling lines, and two of four brushholders can be seen. Part of the brush load current supply is also visible in the upper left of the photograph. A close-up view of a brushholder, inserted brush, and the mechanical load spring is shown in Fig. 2.4. Water coolant feed lines are visible on the left, and a proximity ring vibration sensor is shown to the right side of the photograph.

Figure 2.1: Machine Environment Brush Tester (MEB)
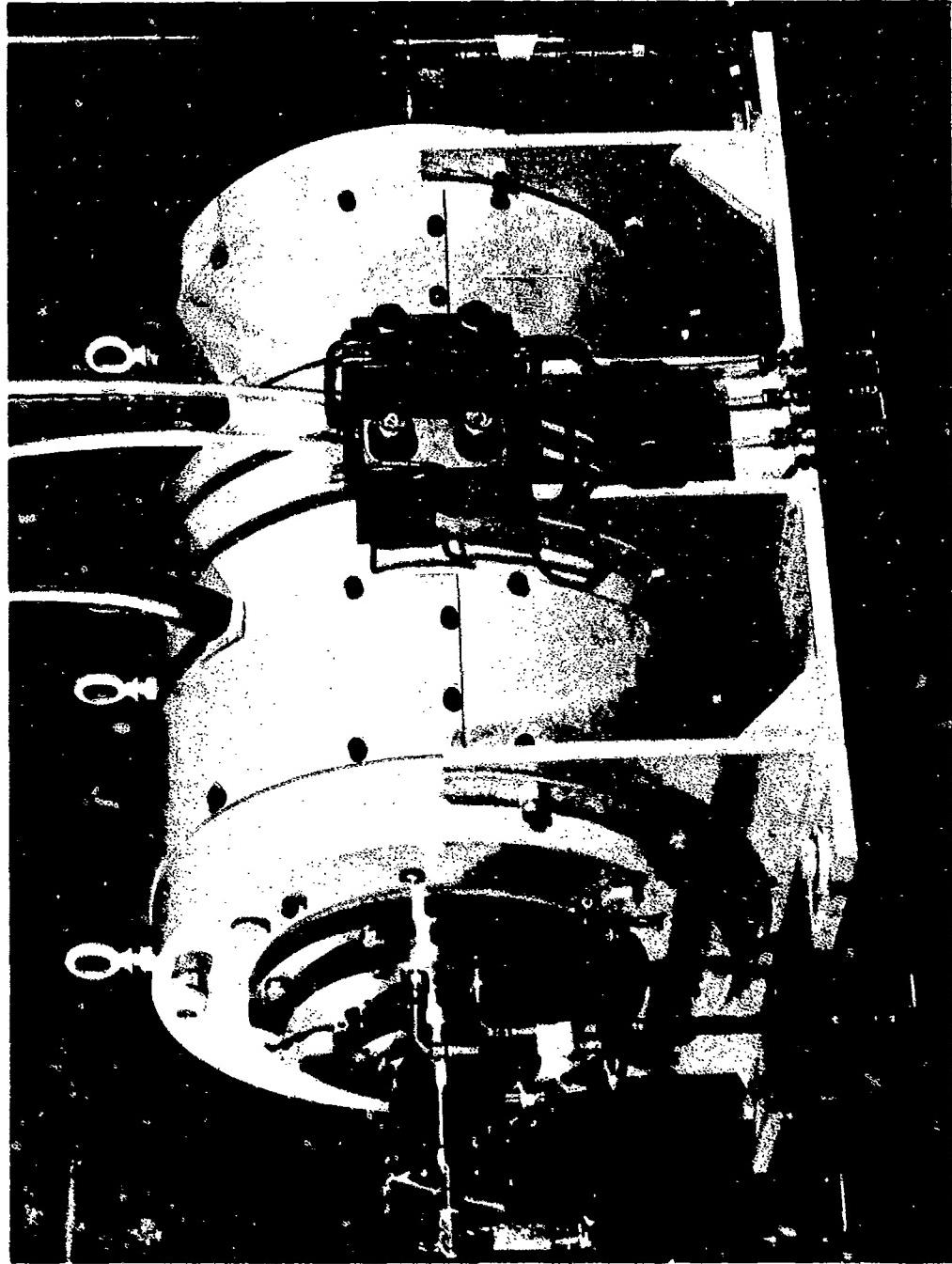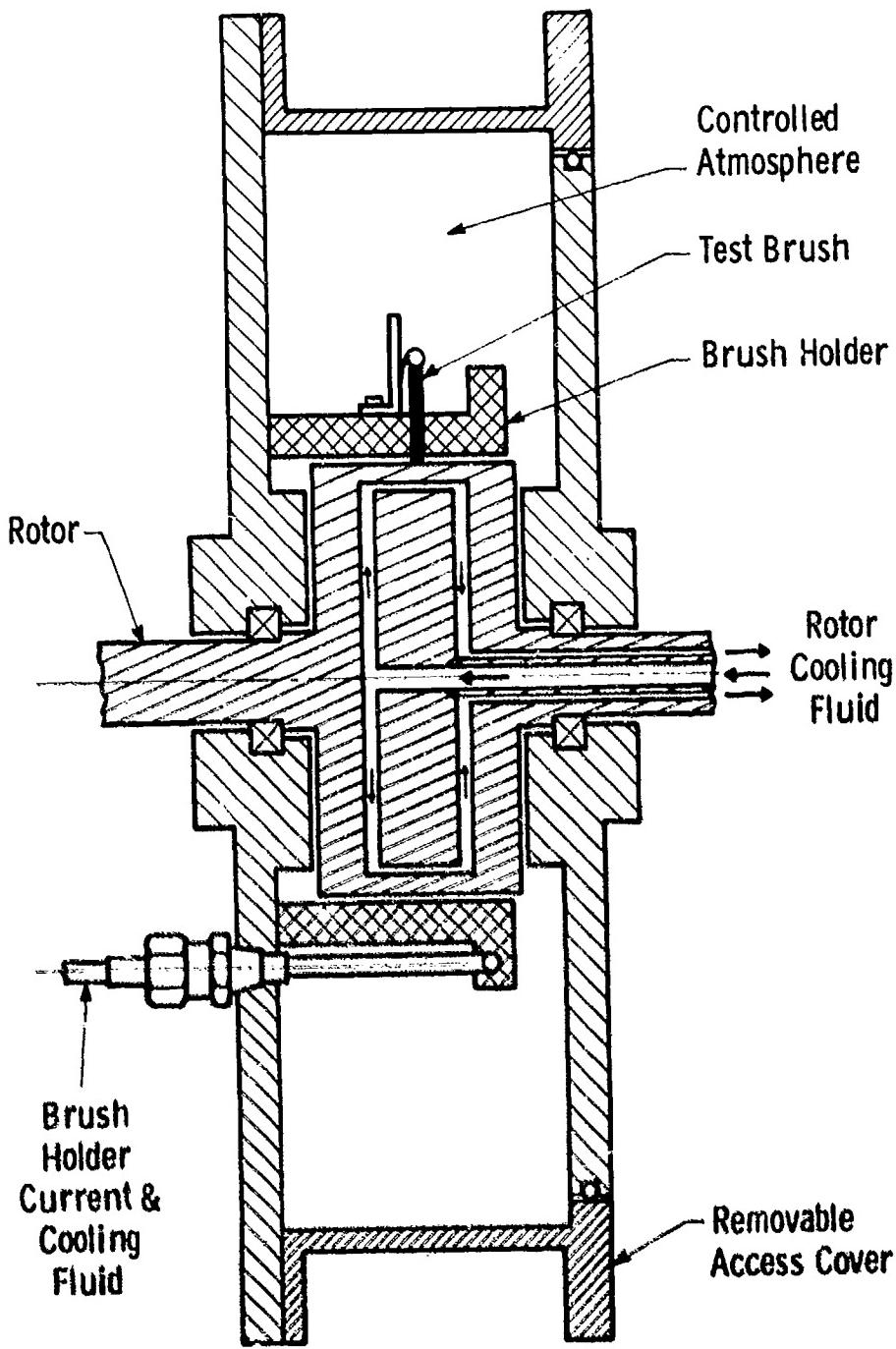
Figure 2.2: Advanced Brush System Test Stand (ABS)
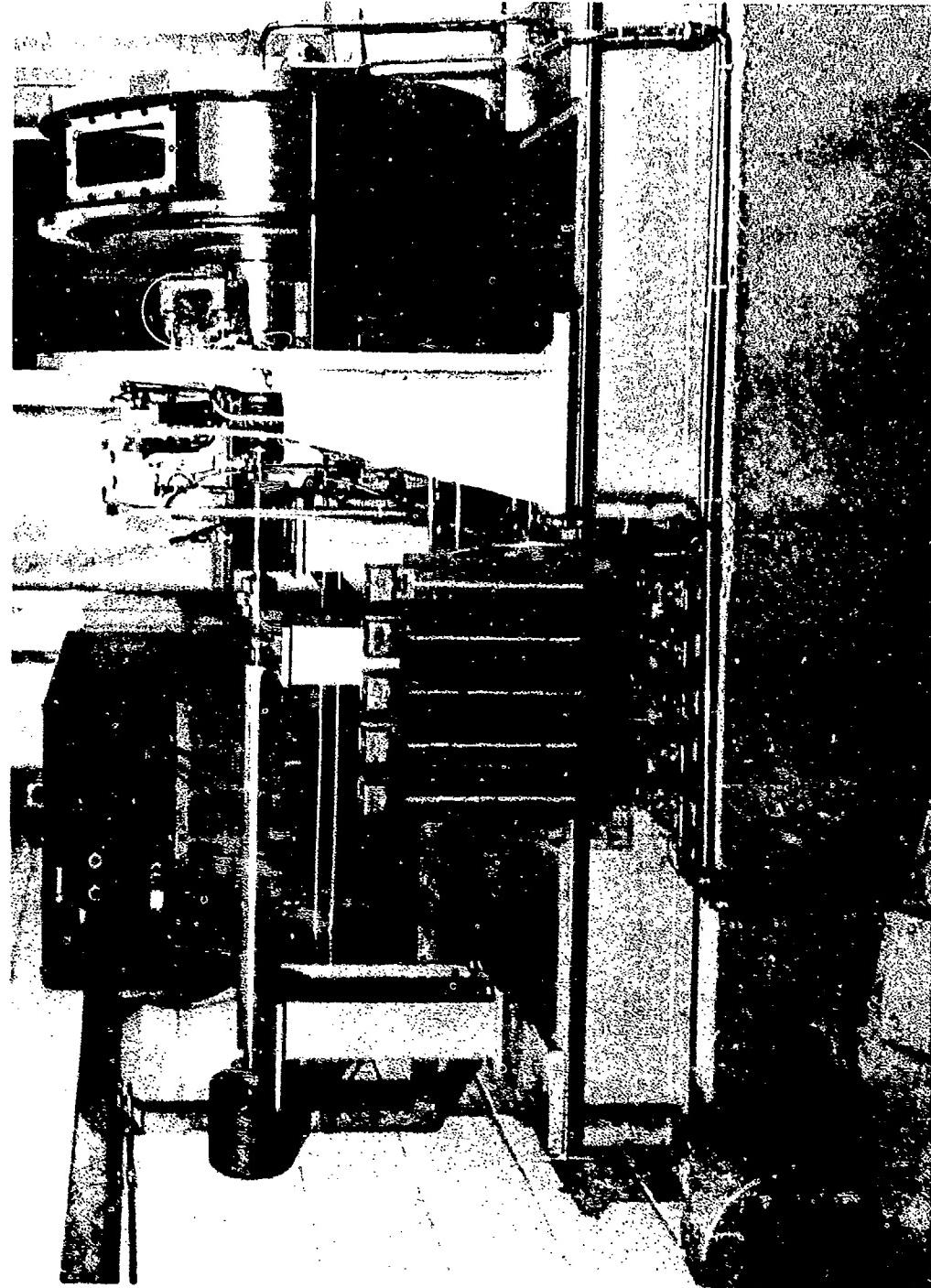
Figure 2.3: Advanced Brush System Test Stand (ABS)
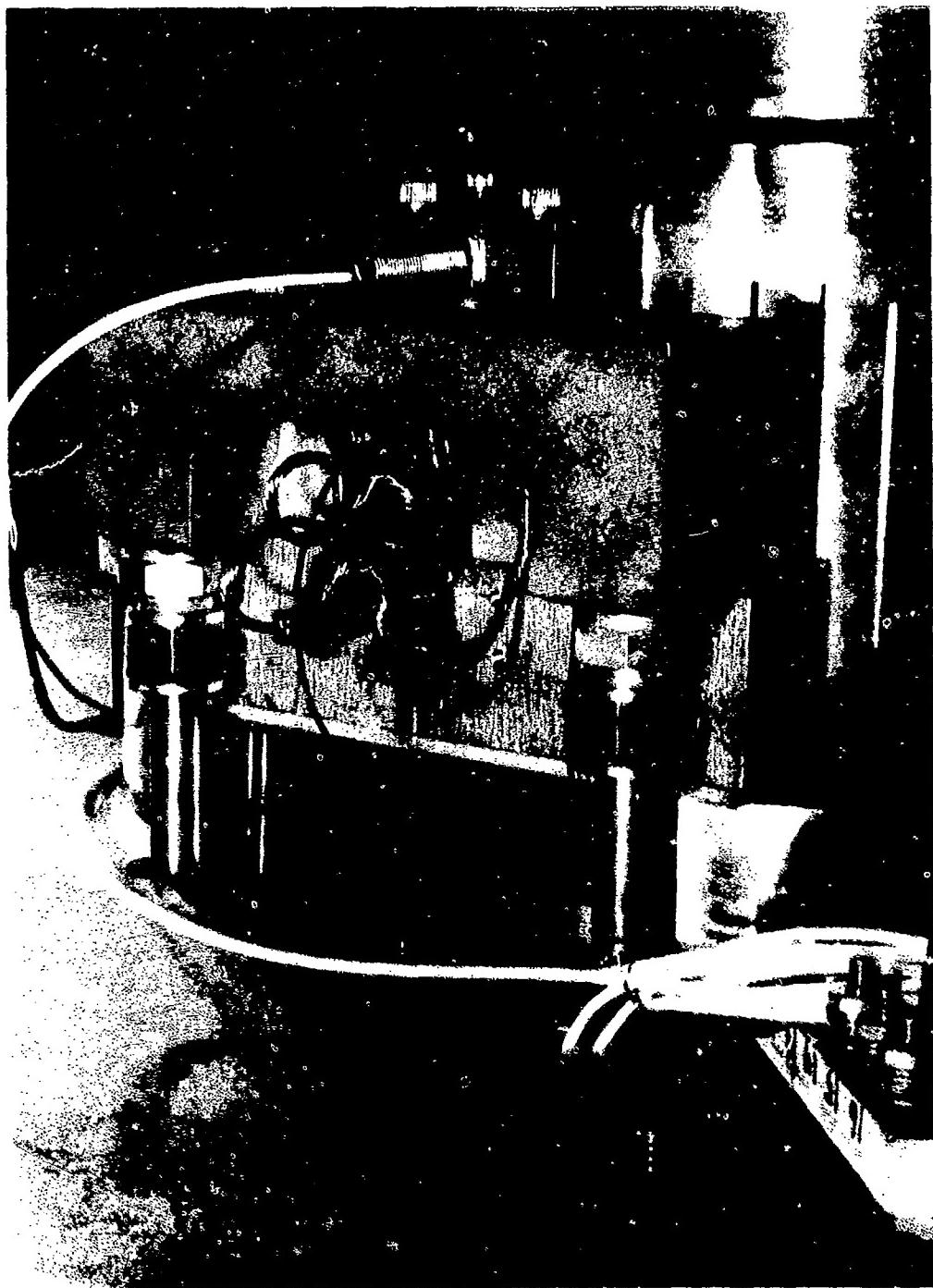
Figure 2.4: ABS Brushholder Arrangement

RM-71132

SECTION 3

CURRENT COLLECTOR MATERIAL PERFORMANCE

3.1 OBJECTIVES

The objective of this task was to select brush and slipring materials for sliding contacts in advanced electromechanical machines. Important system requirements are high current density capability, low interface energy loss, and long life (see Section 1).

3.2 PRIOR AND RELATED WORK

Results of recently completed screening tests of commercially available graphite and metal-graphite brushes, representing a wide percentage weight range in metal content (0-97 w/o), and selected metal sliprings were previously reported (ARPA Contract DAHC 15-72-C-0229, Final Technical Report for Contract from 10 May 1972 through 30 June 1976). The tests were conducted in a humidified carbon dioxide atmosphere, with typical operating conditions of 80 A/cm^2 (10 times the conventional brush current density), 25 m/s ring speed, and 80 kPa mechanical load.

In general, the performance characteristics of copper- and silver-graphite brushes of comparable processing and metal content and running on copper sliprings were found to be similar. Total contact energy loss (energy density per unit slide distance) was a minimum when the brush metal content was near 75 w/o (1.5 J/cm^2.m). The energy loss was dominated by the electrical loss component when the metal content was less than about 70 w/o, but mechanical losses dominate at larger metal contents. Brush wear (volume wear per unit slide distance)

3-1

was very low (0.5 mm^3/Mm), for small additions of metal, increasing at a modest rate up to about (3.2 mm^3/Mm) at 75 w/o. At higher metal percentages the brush wear increased sharply.

Selected sliprings of copper, nickel, and steel were evaluated in combination with copper-graphite brushes containing relatively low copper contents. The lowest total energy loss was obtained with copper rings; increasing losses occurred when the copper ring was replaced with nickel, and even more with a steel ring. This is attributed to the higher contact resistance associated with the latter two materials, although their respective friction coefficients were lower than that for the copper ring. Long brush life was obtained for each of the three ring materials evaluated.

3.3 CURRENT PROGRESS

The work reported here was designed to assess the influence of material substitution on high current brush-ring electrical sliding contacts. The results have led to the selection of several promising, readily available elements of the contact system for further detailed assessment. The optimum contact system for advanced electrical machines of the SEGMAG type may ultimately involve more exotic materials or methods of construction which are specifically tailored to meet the machine requirements. Four commercially available brush materials have been identified as candidates for subsequent advanced testing in the ABS and MEB test rigs. These materials include three silver-graphites formulated by a powder metallurgy technique and containing 64 to 80 weight percent silver, and one copper-graphite with about 37

3-2

weight percent copper which was added to the graphite structure by an infiltration process. From the nineteen slipring materials tested during this period, high strength-high conductivity copper alloys and silver-surfaced metals are considered to be the best candidates for the high current contact system.

3.3.1 Brush Materials

In previous work, commercially available brush materials were screened to identify the most promising candidates for further high current tests. From a substantial number of candidate materials supplied by three vendors, three metal graphite grades were found to be worthy of further consideration. These brush material grades are identified as SG216, SG142, and DM806. The first two grades are formulated by a powder metallurgy technique and they contain relatively high weight percentages of silver metal. The third grade contains a relatively low percentage of copper, which was added to the graphite matrix structure by another manufacturing process.

During this period then additional brush materials were tested, of which only one may be considered as a future test candidate, SG156. This material is similar to the above mentioned silver-graphite grades, but is alleged to contain somewhat less silver by weight. A summary of the performance characteristics of the selected candiate material brushes, as determined under the screening test conditions, is shown in Table 3.1.

TABLE 3.1

PERFORMANCE OF SELECTED BRUSH GRADES

(B1 Screening Tester)

Single Brush Area 1 cm^2 Carbon Dioxide Atmosphere
Two Brushes Per Set   Moisture Additive
Current Density 78 A/cm^2 Copper Slipring
Load Pressure 83 kPa   Ring Velocity 13 m/s

Brush Grade	Nominal Metal Content w/o	Number of Runs	Single Brush Drop, V	Friction Coef., μ	*Energy Loss Density $J/cm^2.m$	Brush Holder Temp., °C	*Brush Wear, mm^3/Mm
SG216	80	11	.019	.18	1.61	67	11.36
SG142	75	2	.012	.23	1.92	72	3.24
SG156	64	1	.018	.19	1.78	74	1.20
DM806	37	7	.11	.18	2.14	86	0.23

*Goals:

	Loss	Wear	Velocity	Current Density
Generator	1.14	2.53	70	155
Motor	1.24	4.86	37	155

The above data serves as an aid in selecting, from available brush materials, the best ones for subsequent advanced testing and final choice for the demonstration SEGMAG machines. Their performance in such machines may not be fully anticipated from the present results, since the final operating conditions will differ in several important respects. For example, in the demonstration machines the rings and brushholders will be force-cooled, and lower operating temperatures, which favor the surface adsorption of gases and vapors, may extend the current carrying capacity and speed range of the brush-ring contacts.

Additionally, the many parallel brushes required for machine operation will have an effect on the ring film formation, again influencing contact performance. Thus a different ranking of the candidate materials, in terms of interface energy loss and brush life, may ultimately be found when future evaluations are made at higher speeds and current densities. Nevertheless, the present materials are likely to point towards the optimum metal/graphite ratios.

The results of testing three of the initially selected candidate material brushes at higher speeds and higher current densities in a different test rig are shown in Table 3.2.

TABLE 3.2

PERFORMANCE OF SELECTED BRUSH GRADES

(HS1 Tester)

Single Brush Area 1.26 cm^2 Carbon Dioxide Atmosphere
Four Brushes/Set   Moisture Additive
Separate Polarity Tracks   ZrCu Alloy Slipring
Load Pressure 103 kPa

Brush Grade	Ring Velocity, m/s	Current Density, A/cm^2	Single Brush Drop, V	Friction Coef., μ	Energy Loss Density, $J/cm^2 \cdot m$	Brush Holder Temp., °C	Brush Wear, mm^3/Mm
SG216	25	78	.08	.14	1.71	70	6.37
SG216	25	155	.19	.08	1.97	83	7.00
SG216	51	155	.09	.12	1.53	85	17.76
SG216	25	233	.15	.11	2.48	94	10.45
SG142	25	78	.11	.15	1.89	67	4.30
SG142	25	155	.21	.10	2.30	84	4.11
SG142	51	155	.11	.12	1.59	81	13.56
DM806	25	78	.14	.16	2.10	81	0.34
DM806	51	78	.20	.15	1.86	105	0.23
DM806	25	116	.26	.11	2.34	103	0.30
DM806	25	155	.50	.13	4.41	150	Dusted

Relative to the current density and speed ranges explored, overall energy loss and wear performance data are noted. The energy loss density increases with increasing current density, but decreases with increasing speed. The net effect, from these experiments, is that the energy loss decreases with simultaneous or combined increases in current density and speed. Brush wear, however, tends to increase with both current density and ring speed. Brush grade DM806 exhibited very low brush wear, except for the highest current density, where dusting occurred. This may be attributed to the high operating temperature which occurred in this case with uncooled brushes and which leads to surface vapor desorption, loss of lubricity, and high wear. Forced-cooling, which will be available in the advanced brush test rigs and the demonstration machines, is likely to forecast such brush behavior.

3.3.2 Ring Materials

Testing of slipring materials continued during this period, utilizing the bench-type laboratory brush test apparatus. As before, the tests were conducted in a humidified carbon dioxide environment. Typical screening operation conditions were used and the selected slipring materials were evaluated, in combination with copper-graphite grade DM806 brushes. The ring materials included copper, silver, high strength-high conductivity copper alloys, graphite, nickel, nickel alloys, high zinc brass, and steels. A summary of the operating conditions and test performance results for each slipring material is shown in Table 3.3.

Generally, lowest net power loss and longest life were achieved when the test brushes were run on copper, super-strength copper alloys,

and silver-surfaced collector rings. Although lower friction coefficients accompanied operation on nickel, high nickel-containing, and steel metal rings, the associated higher contact resistances resulted in relatively high total energy losses. KR monel appeared to be an exception, combining low contact drop and medium friction losses to yield a low total energy loss and low brush wear. The life of the test brushes was significantly lowered when they were operated on steel or high zinc brass rings.

TABLE 3.3

PERFORMANCE OF SELECTED SLIPRING MATERIALS

(B2 Screening Tester)

Single Brush Area 1 cm^2 Carbon Dioxide Atmosphere
Two Brushes Per Set   Moisture Additive
Current Density 78 A/cm^2 Ring Velocity 15 m/s
Load Pressure 83 kPa   Brush Grade DM806

Slipring Material	Single Brush Drip, V	Friction Coef., μ	Energy Loss Density, J/cm^2.m	Brush Holder Temp., °C	Brush Wear mm^3/Mm
Grade C. Steel	.74	.14	4.86	157	1.72
K Monel-S	.82	.09	4.82	169	<0.15
316 S/Steel	.74	.10	4.50	165	20.97
35 Zn Brass	.58	.11	3.81	123	2.29
45 Ni/55 Cu	.54	.08	3.34	136	0.55
30 Ni/70 Cu	.53	.08	3.31	136	0.59
#3 Tool Steel	.39	.15	3.15	119	13.20
Monel	.49	.07	3.00	127	0.99
Nickel	.38	.10	2.73	108	0.25
Graphite	.26	.13	2.36	96	0.10
Ag plated Cu	.14	.18	2.17	97	0.20
Zr Cu	.07	.21	2.05	92	0.20
15 Ni/85 Cu	.12	.17	2.00	90	0.40
Cu (Ag bearing)	.10	.19	2.00	85	<0.15
8 Sn/4 Zn/Cu	.07	.20	1.98	93	0.20
Cupaloy	.11	.17	1.97	88	0.20
OFHC Cu	.07	.19	1.91	92	0.30
PD 135 Cu	.06	.19	1.85	90	<0.15
KR Monel	.13	.15	1.82	92	0.25

SECTION 4

CURRENT COLLECTOR LOADING SYSTEMS

4.1 OBJECTIVES

The objective of the current collection system is to transfer electrical power between stationary and rotating contact members efficiently, reliably and with long life. The loading system is the portion of the current collector that is accountable for controlling the brush electrical, thermal and mechanical loads to acceptable values. The contact material performance program will determine the desired brush loading, and the current collector loading system program will determine how to achieve these requirements.

4.2 PRIOR AND RELATED WORK

High current density brush holders were designed and built for the (HS1 and HS2) High Speed Test rigs. These brush holders were the result of efforts to obtain an immediate test vehicle. The design configuration consisted of a water cooled holder surrounding a rectangular shaped solid brush, constant force springs and conventional (pigtail) electrical shunts to provide a low resistance current path.

Brush holders were designed and built for the Machine Environment Brush Tester (MEB). The design philosophy was similar to that used for the High Speed Testers.

In the area of cooling, however, the design configurations differ. Both machines exhibit water cooled brush holders, but only the MEB has a water cooled rotor.

4-1

The ability of fiber brush shunts to transfer high density current through the solid brush and into the stator conductor was proven.

4.3 CURRENT PROGRESS

4.3.1 Electrical Shunt

4.3.1.1 General

The electrical shunts have progressed through two generations of development. The first generation shunt was described in the final report of a contract submitted to ARPA in September 1976. This shunt configuration was composed of circular brass fibers drawn into brass blocks and then silver plated. The bundles of brass fibers were found to be too stiff and, as a result, only a fraction of the fibers carried the current. A second generation shunt was developed to obtain a more flexible contact. The second generation shunt performance, as well as the supporting theory, is presented in this report.

4.3.1.2 Theory

The theory of the fiber shunt is divided into three areas:

- electrical
- thermal
- mechanical

4.3.1.2.1 Electrical

The electrical resistance of the fiber shunt consists of contact, fiber body and fiber holding bracket resistances. The contact resistance is:

$$r_c = \frac{c}{(f)^k} \text{ , ohm} \qquad (4.1)$$

where

r_c = single contact resistance, ohm

f = single contact load, N

c = constant, ohm $(N)^k$

k = constant, dimensionless

If one assumes a number of equal contacts arranged electrically in parallel, the total contact resistance is:

$$R_c = \frac{r_c}{n} \text{ , ohm} \qquad (4.2)$$

where

R_c = total contact resistance, ohm

n = number of contacts

and

$$F = nf, \text{ N} \qquad (4.3)$$

where

F = total force

Combining equations 4.1, 4.2 and 4.3 yields the total contact resistance as a function of the total contact force.

$$R_c = \frac{c}{n^{1-k} (F)^k} \text{ , ohm} \tag{4.4}$$

The electrical resistance of the fiber body is:

$$r_b = \frac{\rho \ell}{a} \text{ , ohm} \tag{4.5}$$

where

r_b = body electrical resistance, ohm

ρ = material electrical resistivity, ohm

ℓ = fiber length, m

a = fiber cross-sectional area, m^2

For fibers that are plated, the composite body resistance is:

$$r_b = \frac{\rho_1 \rho_2 \, \ell}{a_1 \rho_2 + a_2 \rho_1} \text{ , ohm} \tag{4.6}$$

where subscripts 1 and 2 represent respective composite materials.

$$a_1 = wt, \, m^2 \tag{4.7}$$

where

a_1 = cross-sectional area of fiber inner material, m^2

w = fiber width, m

t = fiber inner material thickness, m

$$a_2 = w(T-t), \text{ m}^2 \qquad (4.8)$$

where

a_2 = cross-sectional area of fiber plating material, m^2

T = fiber composite thickness, m

The total body resistance for a number of equal fibers arranged electrically in parallel is:

$$R_b = \frac{\rho_1 \rho_2 \, \ell}{n(a_1 \rho_2 + a_2 \rho_1)} \qquad (4.9)$$

where

R_b = total body electrical resistance, ohm

The electrical resistance of the fiber holder bracket is:

$$R_H = \frac{\rho_H \, L}{A_H} \text{ , ohm} \qquad (4.10)$$

where

R_H = fiber holder bracket electrical resistance, ohm

ρ_H = bracket at material electrical resistivity, ohm - m

L = mean bracket length, m

A_H = bracket cross-section and area, m^2

4.3.1.2.2 Thermal

The thermal characteristics of the electrical shunt fibers are based on the following assumptions:

1. All of the fiber shunt electrical loss is conducted through the shunt, i.e., no shunt loss goes into the brush.

2. All of the fiber shunt electric loss including body and contact loss is generated at the contact.

3. The thermal resistance of the fiber holding bracket is negligible.

The power loss in the fiber shunt is:

$$P = I^{2'}(R_c + R_b + R_H) \qquad (4.11)$$

where

P = total power loss, watt

I = total shunt current, amp

The conductive heat transfer through the shunt is:

$$Q = \frac{\Delta T}{R_T} \text{ , watt} \qquad (4.12)$$

where

Q = shunt heat transfer, watt

ΔT = temperature difference between brush and brush holder, °C

R_T = shunt thermal resistance, °C

The fiber thermal resistance is:

$$r_t = \frac{\ell}{ak} \text{ , °C/watt} \qquad (4.13)$$

where

r_t = fiber thermal resistance, °C/watt

k = thermal conductivity, watt/m°C

4-6

For a composite fiber, the thermal resistance is:

$$r_t = \frac{\ell}{a_1 k_1 + a_2 k_2} \, , \, °C/watt \qquad (4.14)$$

where subscripts 1 and 2 represent respective thermal paths.

The total thermal resistance for a number of composite fibers arranged thermally in parallel is:

$$R_T = \frac{r_t}{n} \, , \, °C/watt \qquad (4.15)$$

where

R_T = total thermal resistance, °C/watt

Combining equations 4.11 and 4.12 by conservation of energy and solving for current yields:

$$I = [\frac{\Delta T}{R_T(R_c + R_b + R_H)}]^{0.5} \, , \, amp \qquad (4.16)$$

where

I = maximum allowable current per fiber shunt, amp

4.3.1.2.3 Mechanical

The fiber contact loading effect on the solid brush is one of the major considerations in the shunt design. In order for the solid brush to move radially in and out of the brush holder with rotor movement, the shunt-to-brush friction must be overcome. In the brush-to-slipring interface loading, the allowable variation has been stipulated by the Brush Material Performance program as a percent of the brush-to-slipring loading.

4-7

The allowable shunt load is:

$$F = \frac{\% \, F_B}{100(\mu_s + \mu_B)} \; , \; N \qquad (4.17)$$

where

F = allowable shunt load, N

% = allowable percentage variation in brush-to-slipring
   loading, dimensionless

F_B = brush-to-slipring loading, N

μ_s = fiber shunt-to-brush coefficient of friction, dimensionless

μ_B = brush-to-holder coefficient of friction, dimensionless

The shunt force (F) in equation 4.17 is a maximum allowable
force. Also, the brush-to-holder coefficient of friction in equation
4.17 could be eliminated if fiber shunts were applied to opposing sides
of the brush. Equation 4.17 is for a fiber shunt loaded on only one
side of a brush.

The fiber shunt is essentially a grouping of cantilevered
springs arranged mechanically in parallel. For a cantilevered beam with
concentrated end loading, the deflection is given as:

$$y = \frac{f \, \ell^3}{3EI} \; , \; m \qquad (4.18)$$

where

y = shunt finger deflection, m

E = modulus of elasticity, N/m^2

I = second moment of area, m^4

The deflection formula for a similar composite beam is:

$$y = \frac{f \ell^3}{3[E_1 I_1 + E_2 I_2]} \text{ , m} \tag{4.19}$$

where subscripts 1 and 2 represent respective composite materials.

$$I_1 = \frac{wt^3}{12} \text{ , m}^4 \tag{4.20}$$

where

I_1 = second moment of area of fiber inner material, m^4

$$I_2 = \frac{w(T^3 - t^3)}{12} \text{ , m}^4 \tag{4.21}$$

where

I_2 = second moment of area of fiber plating material, m^4

Combining equations 4.17 and 4.3 yields an expression for deflection as a fraction of total fiber shunt force:

$$y = \frac{F \ell^3}{3n[E_1 I_1 + E_2 I_2]} \text{ , m} \tag{4.22}$$

The maximum fiber stress occurs on the outermost fibers of either the inner or the outer material depending on the material properties and geometry. The maximum stress in the inner material is:

$$\sigma_1 = \frac{6 F \ell t}{nw[t^3 + (E_2/E_1)(T^3 - t^3)]} \text{ , N/m}^2 \tag{4.23}$$

4-9

where

σ_1 = maximum stress of the fiber inner material, N/m^2

t = thickness of the inner material, m

w = width of fiber, m

The maximum stress in the outer material is:

$$\sigma_2 = (\frac{E_2}{E_1}) \frac{6 F \ell T}{nw[t^3 + (E_2/E_1)(T^3-t^3)]} , N/m^2 \qquad (4.24)$$

where

σ_1 = maximum stress of the fiber outer material, N/m^2

4.3.1.3 Fiber Shunt Test Results

Single point contact electrical resistance tests were performed for silver on silver contacts. A relationship for the electrical resistance as a function of load was determined experimentally for the silver on silver contacts in air. This relationship was used as a design tool since the multi-fiber shunts were to be silver plated and mated to a silver plated surface.

Shown in Figure 4.1 is a photograph of the second generation multi-fiber shunt. This particular shunt has 56 silver plated rectangular cross-sectioned, brass fibers attached to a copper base. The predicted as well as the actual performance of this shunt is shown on Figure 4.2. The predicted performance is based on the design conditions listed in Table 4.1. At a current of 97.5 amps and a total contact load of .58 N (0.13 lb) this total voltage drop is predicted at 0.02 volt.

The experimental results were higher than the prediction by twenty to forty percent. This higher than predicted resistance is believed to be due to an inadequate electrical connection between the fingers and the finger holding bracket. Succeeding generations of multi-fiber shunt have been designed in a manner to make this electrical connection adequate.

4.3.2 Actuation Systems

No work was scheduled or undertaken in this area for the first year of effort. Beginning in June 1977, mock-ups of new actuation concepts developed under previous ARPA and Westinghouse efforts will be constructed.
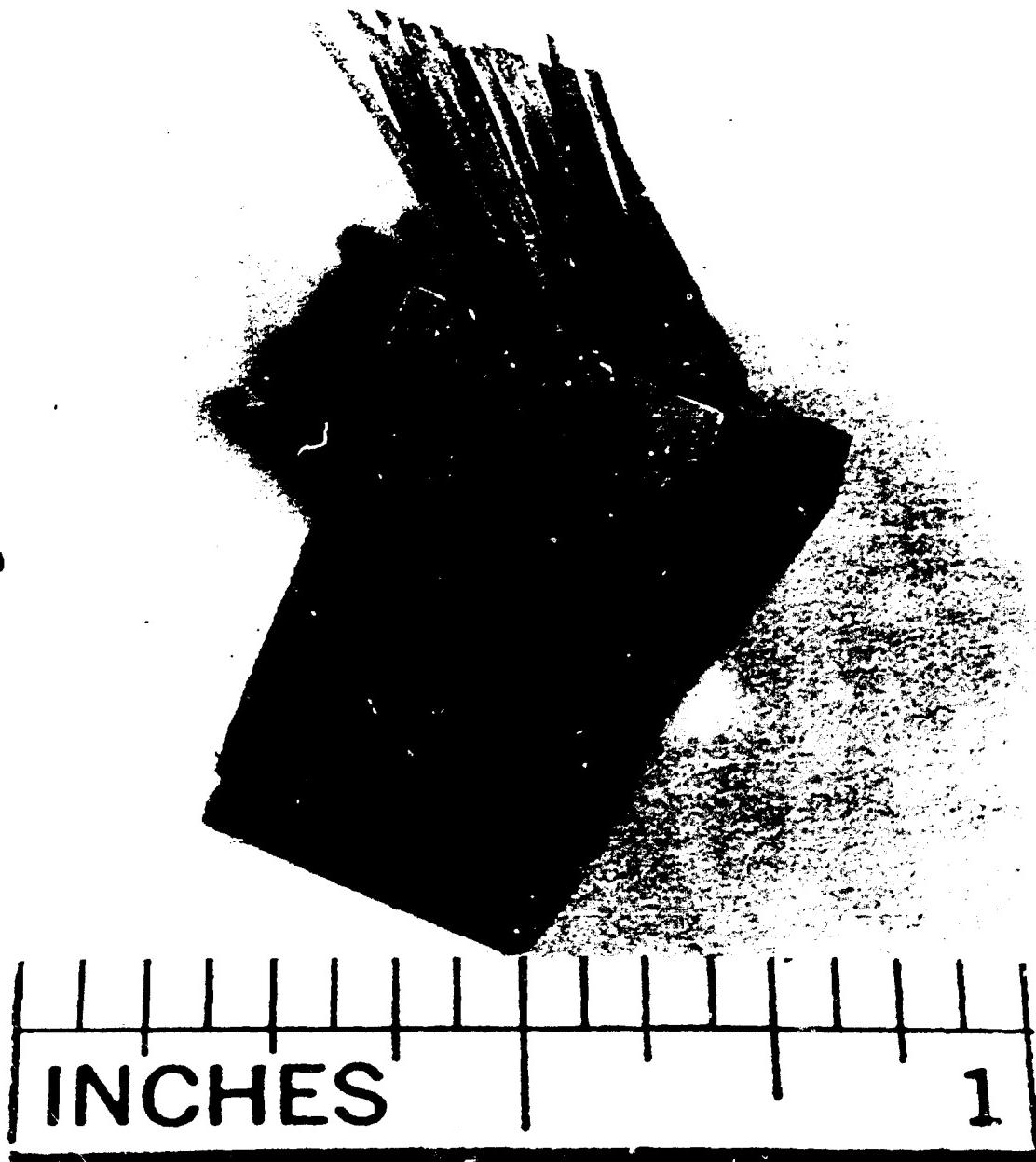
Figure 4.1: Second Generation Metal Fiber Shunt (MFS)
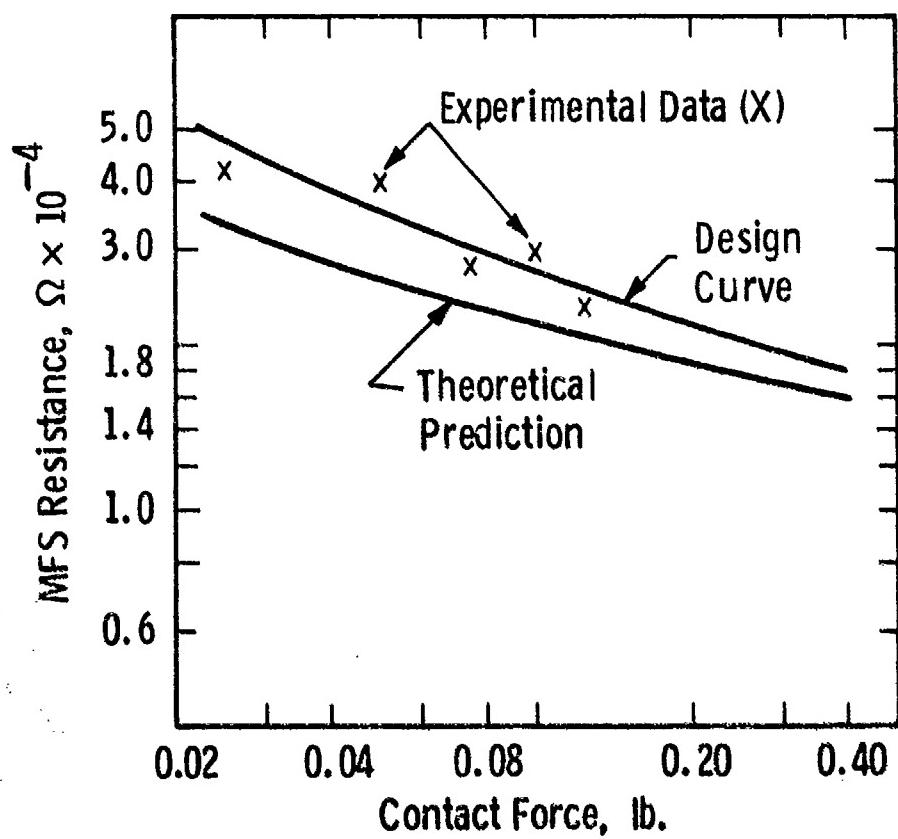
Figure 4.2: Metal Fiber Shunt (MFS) Electrical Performance

TABLE 4.1

MULTI-FIBER SHUNT, SECOND GENERATION
(MFS II) DESIGN CONDITIONS

$w = 1.27 \times 10^{-3}$ m (.05 in.)

$t = 1.27 \times 10^{-5}$ m (.0005 in.)

$T = 3.30 \times 10^{-5}$ m (.0013 in.)

$\ell = 8.89 \times 10^{-3}$ m (.35 in.)

$n = 56$

$A_H = 2.45 \times 10^{-3} m^2$ (.038 in.^{2})

$L = 9.14 \times 10^{-3}$ (.36 in.)

$\% = 5$

$F_B = 7.52$ N (1.69 lb)

$\mu_s = .35$

$\mu_B = .30$

$k = .45$

$c = 8.03 \times 10^{-4}$ Ω - N ($4.1 \times 10^{-4} \Omega$ -lb^k)

$\rho_1 = 6.43 \times 10^{-8}$ (2.53×10^{-6} Ω - in.)

$\rho_2 = 1.60 \times 10^{-8}$ (.63 $\times 10^{-6}$ Ω -m)

$\rho_H = 1.78 \times 10^{-8}$ (.70 $\times 10^{-6} \Omega$ -in.)

$k_1 = 121$ watt/m°C (70 Btu/Hr ft °F)

$k_2 = 431$ watt/m°C (249 Btu/Hr ft °F)

$E_1 = 1.03 \times 10^{11}$ N/m^2 (15 $\times 10^6$ lb/in.^{2})

$E_2 = 7.58 \times 10^{10}$ N/m^2 (11 $\times 10^6$ lb/in.^{2})

SECTION 5

CURRENT COLLECTOR GASEOUS ENVIRONMENT

5.1 OBJECTIVES

The objective of this task was to select gas atmospheres and
vapor additives for use in sliding contacts for advanced electromechanical
machines. Important requirements of these elements are to impart high
current carrying capability, low interface energy loss, and long life to
the brushes and rings.

5.2 PRIOR AND RELATED WORK

The operating performance (contact resistance, friction, and
wear rate) of conventional carbon brushes is known to be dependent on
the application requirements (electrical load, speed, efficiency),
the materials of the contacting members, and the nature of the environment.
The pressure and composition of ambient gases, including additives such
as water vapor, also play an important role in reducing brush friction and
wear. Organic vapors, particularly vapors of the lower members of the
n-paraffinic hydrocarbon group (n-propane to n-heptane) can substitute
for water vapor. Lubrication of this type is associated with adsorption
of the vapor on the graphite crystallites in such a way that edge-based
plane interactions of these crystallites, which subsequently lead to high
sliding friction, can be eliminated or reduced in the surface films
(see Section 7).

In the search for a gaseous environment which would yield an improved high current brush-ring contact system for SEGMAG-type machines, a number of non-oxidizing gases with moisture additions and several hydrocarbon vapor additives to a carbon dioxide atmosphere were evaluated during this reporting period.

5.3 CURRENT PROGRESS

Five non-oxidizing gases were evaluated for the high current brush-ring contact system. Brush performance was good in each of the gases tested. An advantage which was observed in argon gas, when compared with carbon dioxide under relatively low-speed screening test conditions, was lost when later runs were made at a higher speed and higher current density. Five different hydrocarbons were tested as vapor additions to carbon dioxide gas atmospheres. Brush performance in these environments was found to be dependent on the hydrocarbon molecular weight and vapor concentration. Equal brush life was achieved with much lower concentrations of hydrocarbon vapors than with water vapor. Additional experiments revealed that brush performance was dependent upon the mechanical load as well as the vapor concentration.

5.3.1 Non-Oxidizing Gases

Preliminary experiments were run to evaluate the effects of five different non-oxidizing gas atmospheres on brush performance. Silver-graphite grade SG 142 brushes were operated in combination with a copper slipring under screening test conditions in each of the gases. The test gases included carbon dioxide, sulfur hexafluoride, nitrogen, helium and argon. Water vapor humidification was employed.

5-2

Brush performance in each of the five gases tested was good under the relatively low-speed (13 m/s) screening test conditions. A very low friction coefficient (0.06), the lowest energy loss (1.5 $J/cm^2 \cdot m$) and the lowest wear (0.7 mm^3/Mm) were measured when the test brushes were run in argon. Brush contact voltage drop was very low (0.03 V) in carbon dioxide, but was six to nine times higher in the other gases. The low contact voltage achieved with carbon dioxide, however, was offset by a higher coefficient of friction (0.18) and higher brush wear (3.22 mm^3/Mm). Sulfur hexafluoride was included as a test gas because of its arc quenching and high dielectric strength characteristics.

Additional testing was undertaken with mixtures of carbon dioxide and argon gases to investigate combinations. Silver-graphite grade SG 142 brushes were operated in combination with a copper slipring under the same screening test conditions as those employed with single gases. The advantage of low friction and wear associated with brush operation in argon was progressively lost when the volume fraction of carbon dioxide was increased.

Other tests were conducted with grade SG 142 brushes operating with twice the current density (155 A/cm^2) and twice the speed (25 m/s) in atmospheres of argon or carbon dioxide. From these experiments, the previously shown advantage in brush life (lower wear) when running in argon vs. carbon dioxide was lost. This change in capability may have been caused by the higher operating temperature in the latter case (112° vs. 80°C), possibly adversely affecting gas-moisture adsorption. If this were true, forced cooling of the contact interface surfaces could be expected to alleviate this undesirable effect.

5.3.2 Hydrocarbon and Water Vapor Additives

Experiments were run to evaluate the effect of five different hydrocarbon additives on the performance of silver-graphite grade SG 216 brushes operating in carbon dioxide. The operating conditions, the test vapor additives, and the resulting brush-ring performance characteristics are summarized in Table 5:1. The brush wear which was observed in each of the gas-vapor environments is shown in Figure 5:1. The organic vapor examined included members of the n-paraffinic hydrocarbon group (n-heptane, n-dodecane, and n-hexadecane), one of the corresponding alcohols (heptanol), and a member of the naphthalic group (decalin). Water vapor was also included for reference purposes.

Prevention of dusting wear with high current silver-graphite brushes was achieved by additions of each of the hydrocarbon vapors to the pure dry carbon dioxide operating atmospheres. Moreover, brush wear was reduced by increasing the vapor pressure of the hydrocarbon additives in the range investigated. A given brush life was achievable with lower vapor concentrations as the hydrocarbon molecular weight is increased. For example, equal brush life was observed for 670 and 0.2 Pa vapor pressure of heptane and hexadecane, respectively. A much higher concentration of water vapor, 3000 Pa, was required to achieve the same life.

In contrast to hydrocarbon additives, the brush wear-water vapor curve had a positive slope over the pressure range shown. At some lower moisture pressure, however, the slope will become negative as a transition to high "dusting" wear occurs. The location of all of the brush wear-vapor additive pressure curves will be dependent upon the contact surface

temperature with the curves being likely to shift to the right with increasing temperature as gas-vapor desorption is increased, leading to increased friction and wear.

The data in Table 5:1 shows that significantly higher brush contact voltages prevailed when hydrocarbon additives were substituted for water vapor. The brush voltage increased as the hydrocarbon vapor concentration was increased, but brush-ring friction remained essentially constant, regardless of the vapor additive or its concentration pressure.

The influence of brush mechanical load pressure and moisture vapor concentration on the performance of silver-graphite grade SG 216 brushes operating on a silver-surfaced slipring is shown in Table 5:2. The experiments reported here were undertaken at a current density of 78 A/cm^2, a slipring velocity of 13 m/s, and in carbon dioxide.

As the mechanical load pressure was reduced (from 83 to 34 kPa), the average contact energy loss and brush wear decreased. For each mechanical load, a tendency also existed for the contact energy loss and brush wear to decrease as the moisture additive partial pressure was decreased (from 2700 to 700 Pa).

TABLE 5:1

VAPOR ADDITIVE EFFECT ON BRUSH PERFORMANCE
(B1 Screening Tester)

Single Brush Area 1 cm^2
Two Brushes per Set
Current Density 78 A/cm^2
Brush Grade SG 216

Carbon Dioxide Atmosphere
Copper Slipring
Ring Velocity 13 m/s
Load Pressure 83 kPa

Test Gas Additive*		Single Brush Drop, V	Friction Coeff., μ	Energy Loss Density, $J/cm^2 \cdot m$	Brush Holder Temp., °C	Brush Wear, mm^3/Mm
Vapor	Concentration, Pa					
Water	2670	.02	.18	1.61	67	11.36
Water	610	.04	.16	1.60	70	7.94
n-Heptane	1310	.11	.15	1.90	70	9.31
n-Heptane	92	.06	.15	1.61	65	22.71
n-Dodecane	15	.12	.16	2.08	75	3.28
n-Dodecane	5.5	.10	.15	1.87	72	4.73
n-Dodecane	.32	.07	.15	1.67	70	18.56
n-Hexadecane	.20	.08	.16	1.93	73	11.89
cis-tran Decalin	43	.10	.16	1.95	73	6.19
cis Decalin	27	.09	.16	1.89	73	9.24
Heptanol	7.3	.10	.15	1.84	78	3.03

*Approximately one atmosphere total gas pressure.

TABLE 5:2

INFLUENCE OF LOAD PRESSURE AND MOISTURE CONCENTRATION
ON A SELECTED BRUSH-RING MATERIAL COMBINATION

(B1 Screening Tester)

Single Brush Area 1 cm^2 Carbon Dioxide Atmosphere
Two Brushes per Set   Silver-Plated Copper Slipring
Current Density 78 A/cm^2 Ring Velocity 13 m/s
Brush Grade SG 216

Mech. Load Press., kPa	Inlet Gas Moisture Conc., Pa	Single Brush Drop, V	Friction Coeff., μ	Energy Loss Density, $J/cm^2 \cdot m$	Brush Holder Temp., °C	Brush Wear, mm^3/Mm
83	2700	.074	.19	2.02	85	7.73
83	700	.075	.17	1.94	81	2.90
69	700	.088	.19	1.83	88	2.90
34	2700	.18	.23	1.88	84	2.53
34	700	.15	.20	1.60	78	2.17
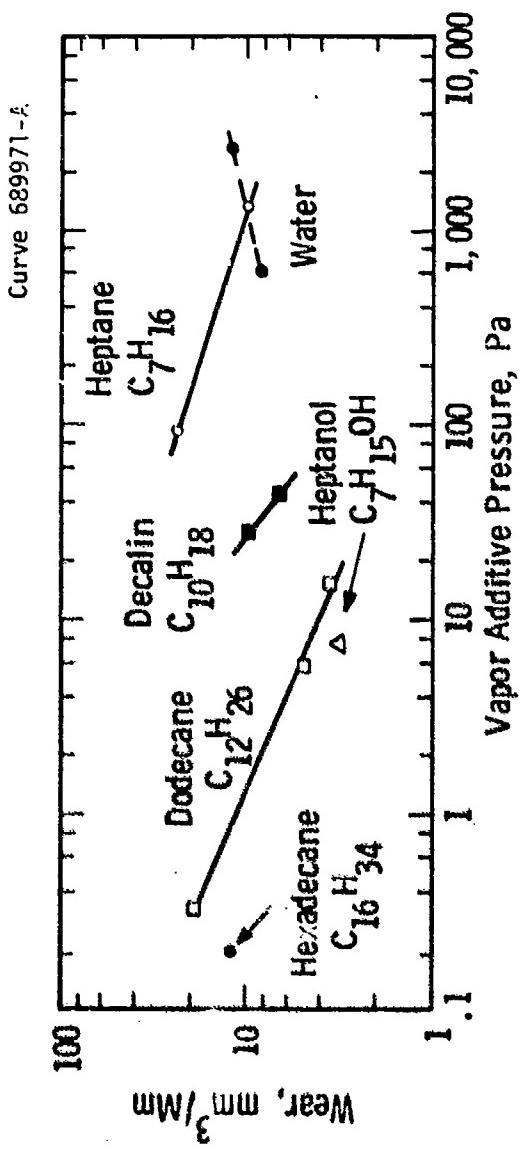
Figure 5.1: Grade SB216 Brush Wear in CO_2 with Vapor Additive

FIBER BRUSH RESEARCH

6.1 OBJECTIVES

This task is intended to establish the nature of the contact and current transferring phenomena involved in the operation of fiber brushes at high current densities and to explore the utilization of these brushes in electromechanical machines.

The main subtasks during this period were:

- to establish techniques for coating fibers with metal
- to fabricate brushes using such fibers
- to establish a fiber brush test rig
- to test fiber brushes on the test rig

6.2 PRIOR RELATED WORK

During the last few years, a new type of brush has been developed employing carbon fibers in a type of construction which enables each fiber to flex individually, so as to conform to the slipring surface. The basic advantage of this brush is that, unlike a solid brush, a large number of electrically parallel, but individually sprung, contacts up to 500,000 per cm^2 are employed.

In the unplated form, carbon fiber brushes, operated in parallel with solid brushes, have enabled commutation to be improved in certain machines. Metal plated carbon fiber brushes, on the other hand, have shown excellent high speed and high current density performance, with low wear rates, brush noise and voltage drops. The exceptionally low

6-1

brush pressure ($\sim$ 7 kPa), by conventional solid brush standards, potentially enables low friction power losses to be achieved.

In prior work, plated fiber brushes have been operated at speeds up to 100 m/s and current densities up to 1.55 MA/m^2, while in the USA, similar brushes have been operated to 360 m/s and 2.8 MA/m^2 during recent pulsed experiments, with considerable success. This is the highest speed achieved with any brush tested to date. Low wear rates have also been achieved with metal coated fiber brushes, particularly with negative polarity brushes, where non-dimensional linear wear rates as low as 2×10^{-12} have been observed during operation in air.

6.3 CURRENT PROGRESS AND FUTURE GOALS

The fiber brush program may be conveniently divided into the areas of metallization of carbon fiber, fiber brush construction, and fiber brush testing. Sufficient progress has been made in the first two areas to yield several pairs of metallized carbon fiber brushes. To date, only one pair has been tested for any length of time (600 h), but results of these tests in various atmospheres at current densities up to 0.78 MA/m^2 were quite encouraging. Future effort will be directed towards more detailed investigations into the operating characteristics, of multiple fiber brushes under conditions of speed and current density which more closely approximate values which will be encountered in future machines. Effort will be directed towards improving brush construction techniques and to developing alternative metallizing processes which could permit increased fiber production rates.

6.3.1 Metallization of Carbon Fiber

Several deposition systems have been tested and evaluated. The procedure which yielded fiber with a metallic shell of highest electrical conductivity at minimum thickness and acceptable mechanical properties utilized unique methods of carbon substrate preparation, followed by metal plating with chemically deposited nickel and electrolytically deposited silver. The thickness of deposited metals was held to an acceptable minimum (< 1 μm) to prevent undesirable increases in the friction coefficient for the completed brush.

To date, only batch methods have been utilized for producing metallized fiber. Yields per batch averaged 20,000 fiber-feet, with a maximum of 30,000 fiber-feet. Approximately 60,000 fiber-feet were used to produce each pair of small experimental brushes ($\sim$ 1.3 cm^2 cross-sectional area). Coating techniques which would permit batch yields of 150,000 fiber-feet per run are at present being considered. In the future, continuous methods for metallizing carbon fiber and other fiber materials may be developed, should this prove to be necessary and economically viable.

Methods which have been developed for evaluating metallized carbon fiber fall into two general categories: optical and electrical. Optical methods included quality checking by eye to determine if any relatively large areas of poor metal coverage existed, observation with an optical microscope at 30X to find unmetallized areas on individual fibers, and SEM investigation of representative fiber bundles and cross sections to determine the uniformity of metal coverage. Figures 6.1,a and 6.1,b show samples of fiber having poor and good metal coatings.

Evaluation of the electrical properties of a batch of fiber has been accomplished using a single fiber test which utilizes a known length of fiber held rigidly between two electrical conductors in a gaseous environment. Quality control standards are currently being established utilizing plots of voltage drop versus current flow. The single fiber test has been used to evaluate fiber performance under various cover gases as well as to compare the quality produced by various metal deposition systems. During tests with single metal coated fibers, current densities up to 12 GA/m^2 have been achieved.

6.3.2 Fiber Brush Construction

In the method of construction utilized during this reporting period, approximately 60,000 fiber-feet of metallized carbon fiber was compacted in fiber bundles of 38 mm length, using a specially designed brush construction fixture. Approximately 400,000 individual fibers were compressed into a rectangular cross section of 1.3 cm^2 to yield a theoretical packing factor of 0.25. The effects of variations in the packing factor and cross sectional dimensions have yet to be tested.

Silver plated brush bases were joined to the trimmed ends of the fibers, using low melting point brazes or solders. Several joining alloys have been tested, and several more have been identified for future testing. The brush bases vary in design, depending on whether the brush pair will be cooled by an internal flow of gas, or not. Three brush base designs have been fabricated to date.

6-4

Evaluation of the brush pair has been undertaken before
separation utilizing a static screening test. Voltage drops across
the pair were measured at various currents, yielding data on the base-to-
fiber interface resistances and on the conductivity of the fiber bundle.
Acceptability standards are currently being established for the static
screening test. The brush pairs were separated following the static
screening tests, yielding two brushes having a free fiber length of
approximately 20 mm.

6.3.3 Fiber Brush Testing

A fiber brush test rig has been assembled utilizing an existing
brush tester with redesigned brush actuators, actuator mounting collar,
and additional instrumentation. Presently, it has capability for monitoring
slipring speeds, brush friction losses, positive and negative brush-to-
slipring voltage drops, positive and negative brush current, positive
and negative brush base temperatures, cover gas flow rate, brush cooling-
gas flow rate, and test chamber ambient temperature. Modifications presently
in hand will permit these capabilities to be extended to include the
control and measurement of water vapor in the cover gas and cooling gas,
measurement of oxygen (in PPM) in the test chamber, variability of slipring
tip speed, provision for separate positive and negative brush tracks on the
same slipring, and the capability to test up to four pairs of brushes
simultaneously, with separate current control for each. Figures 6.2, 6.3
and 6.4 show views of the present facility, control unit and data acquisition
system. Tests to date have utilized silver and copper sliprings.

6-5

Preliminary test results have revealed some interesting relationships for uncooled fiber brushes:

- Positive and negative brush voltage drops increased less than linearly for silver sliprings as the current density was increased up to 0.78 MA/m^2. In fact, constant values were approached in several cases at different current densities, depending on which cover gas was employed. These preliminary results are shown in Figs. 6.5,a to 6.5,d for nitrogen, helium, carbon dioxide and air.

- Positive brush voltage drops were consistently higher than negative brush voltage drops at the same current density, the differences being small for brushes running on a silver slipring surface with carbon dioxide cover gas, but larger for other gases and for brushes running on a copper slipring surface.

- As expected, abraiding the slipring surface prior to a test run, to remove surface films and corrosion products, significantly reduced the positive brush voltage drop for brushes running on a copper slipring surface.

- Friction losses remained quite constant with increasing current density for brushes running on a silver slipring surface, but tended to rise for brushes running on a copper slipring surface.

- No measurable wear was observed on the negative brush during operation for 600 h. Damage to the positive brush occurred on one occasion as a result of overheating, requiring the brush (and slipring) surface to be renovated. Other than that, no wear was observed on that brush either.

The goals of future test programs are to determine the effects on brush performance caused by:

- Gas cooling both positive and negative brushes

- Varying the water vapor content in the test chamber cover gas and brush cooling gas

- Operating multiple brushes on early track

- Using separate tracks for positive and negative brushes

- Adding organic vapors to the cover and cooling gases

- Varying the slipring speed up to 70 m/s

- Varying the brush/slipring interface temperature

- Varying the brush packing factor
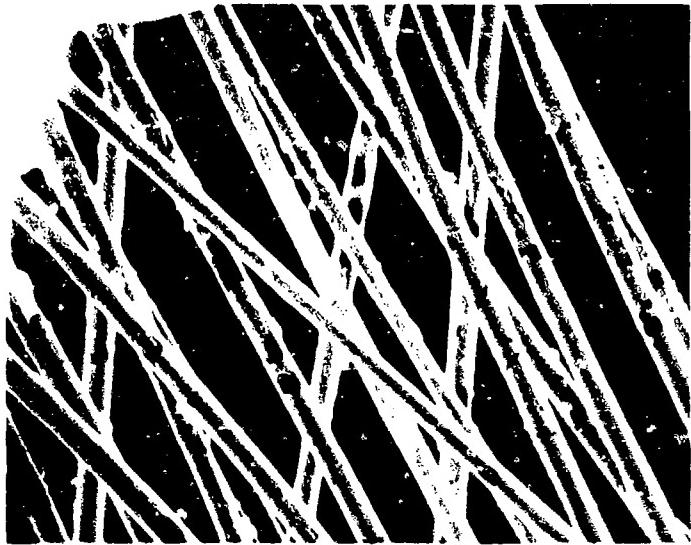
Figure 6.1a: Example of Poorly Plated Fiber
(Au on Panex, 500X)

Figure 6.1b: Example of Fiber with Good Plating
(T15 on Modmor II, 2000X)
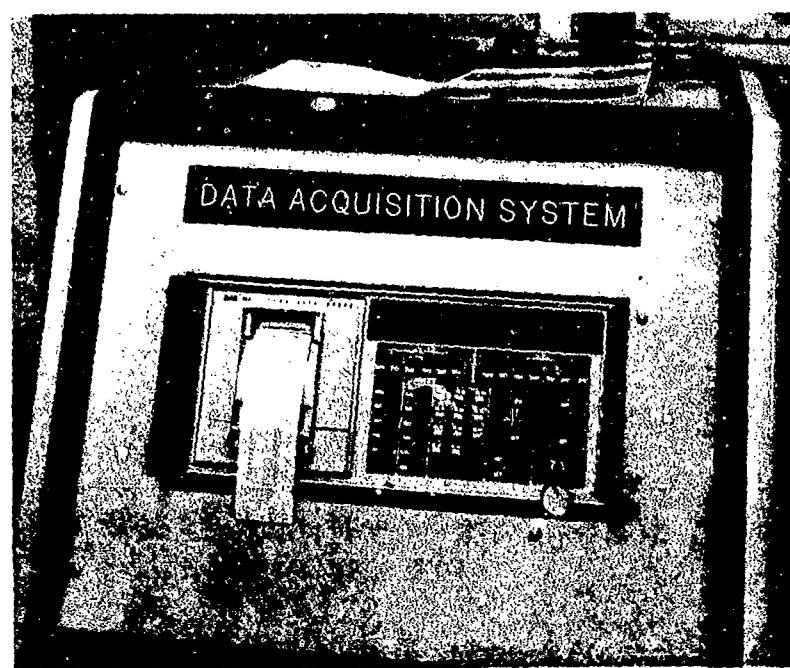
Figure 6.2:   Fiber Brush Test Facility
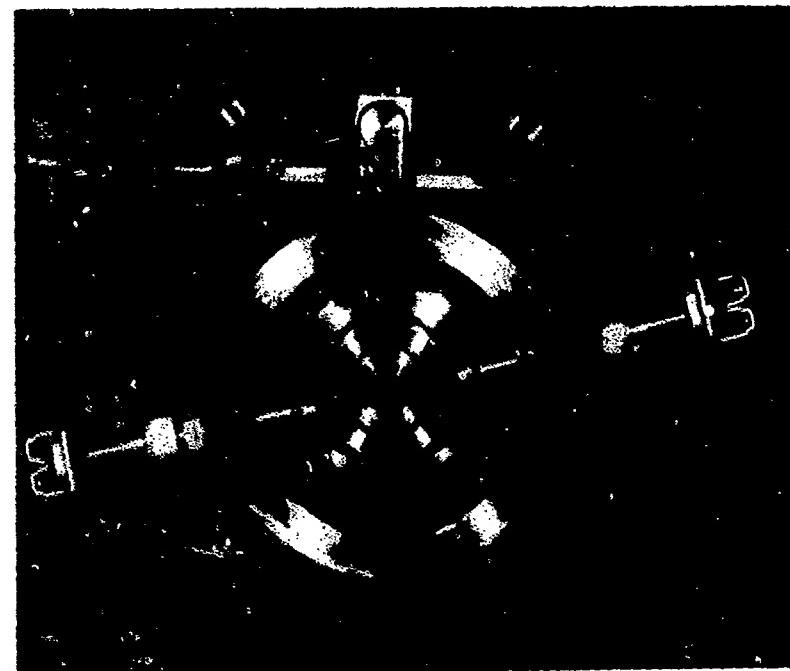
Figure 6.3:   Fiber Brush Test Control Unit
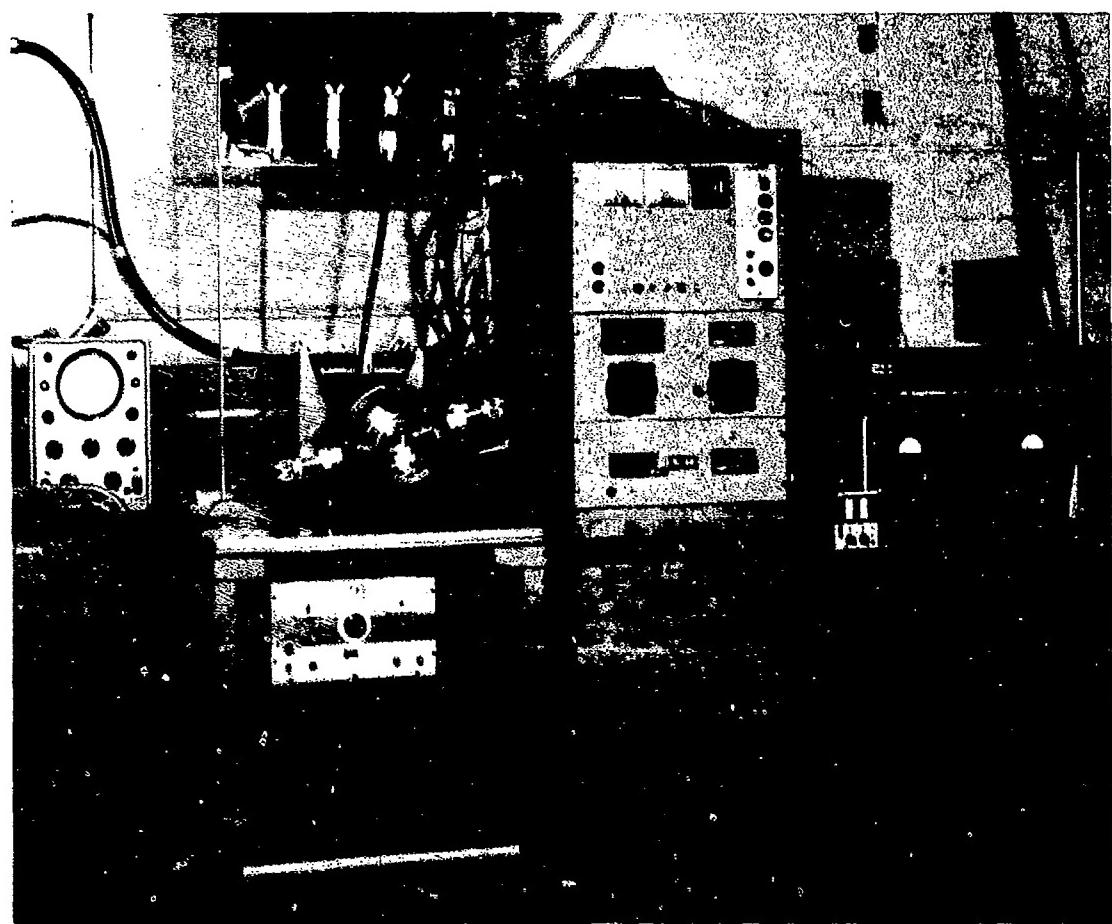
Figure 6.4: Data Acquisition System
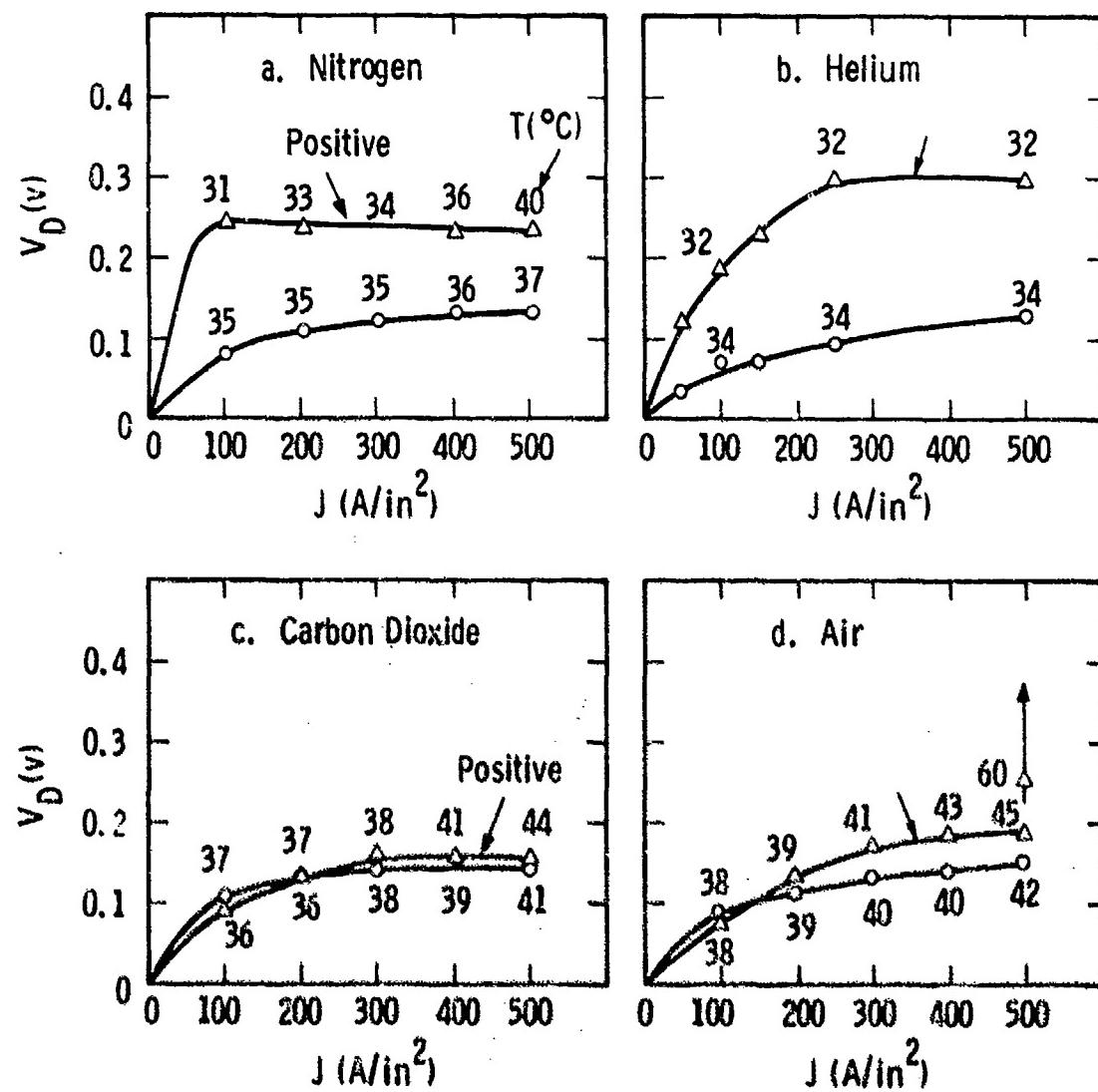
Figure 6.5: Contact Voltage vs. Brush Current for Fiber Brushes
Run on Silver Sliprings in Various Atmospheres

SECTION 7

FUNDAMENTAL RESEARCH PROJECTS

7.1 OBJECTIVES

The objective of fundamental studies on solid-brush current collector processes and systems was to use up-to-date information to develop an understanding of the current transfer process at the brush-sliding surface interface in high current density brushes, so that practical improvements in solid brush performance, mainly low friction, low contact resistance, and low wear rate, can be guided from a firm technical base.

The conventional solid brush for current collection is made of graphite or graphite-metal mixtures, and graphite is widely known as a solid lubricant with a lamellar structure. During this reporting period a literature review was made of the relevant chemical and physicochemical properties of lamellar solids (mainly graphite and dichalcogenides of Mo, W, Nb and Ta, as well as their mixed chalcogenides) and their interaction with metal surfaces. Based on this review and available information about the state-of-the-art of solid brushes, it became apparent that several non-traditional approaches may offer potential benefits in developing brushes having a better performance than those presently available commercially and capable of meeting the demands on brushes for advanced machinery. Various suggestions were outlined and their priorities were assessed for future plans for brush research and development. Based on these priorities, work has recently been initiated in several of the most promising areas.

One of the suggestions was to use long chain n-paraffinic hydrocarbons as vapor additives to substitute for water vapor in the brush operating environment. In parallel with the practical evaluation of brush performance in presence of these vapor additives (see Section 5.3.2), the influence of the hydrocarbon vapors on the electrical resistance of graphite contacts was measured, to provide some understanding of the film resistance of the different hydrocarbon vapors and the voltage drop of the sliding contact system.

7.2 PRIOR AND RELATED WORK

The lubricating properties of graphite in normal atmospheres are well known to be dependent upon the partial pressure of water vapor in the air. Under vacuum, graphite rods or brushes will seize on a moving base (copper or graphite) and wear away rapidly as a fine dust. However, the severe wear under vacuum can be effectively prevented by organic vapors of lower members of the n-paraffinic hydrocarbon group (propane to heptane), by their corresponding alcohols (methanol, 1-propanol), and by halides (carbon tetrachloride, 1-bromopentane) at pressures from several hundreds to less than one-tenth of a newton per square meter, depending on the carbon-chain length of the vapor molecules. The phenomenon of such vapors affecting the lubrication of graphite is generally called "vapor lubrication".

Recent studies of selective adsorption by graphite and molybdenum disulfide indicate that the basal planes (the cleavage faces) of these lamellar solids have a specific affinity for the

7-2

adsorption of n-paraffinic hydrocarbons and also have a capacity to adsorb, preferentially, long chain molecules ($n-C_{32}H_{66}$) from shorter chain ($n-C_7H_{16}$) n-paraffinic hydrocarbon mixtures. The edges of the crystallites have a specific affinity for adsorption of polar molecules such as n-butanol. Such selective adsorption phenomena can be correlated with the surface nature of these lamellar crystallites.

Graphite crystallites are highly anisotropic in their physical characteristics. Low friction occurs when the basal planes are parallel, or nearly parallel, to the sliding surface. As a solid lubricant, the orientation of graphite crystallites in a lubricating film is an important factor in its antifriction and antiwear behavior. When the surface forces of the crystallites are saturated by adsorption of polar or non-polar molecules (water or hydrocarbons) from the environment, the interactions between basal planes and the edges of the crystallites, which cause high friction and wear (as in vacuum), can be prevented or minimized. Thus, vapor lubrication is necessary for graphite to be an efficient lubricant.

The evaluation of vapor lubricants was extended to higher members of the n-paraffinic hydrocarbons which might also be effective lubricants, but which could be employed at much smaller partial pressure because of their larger coverage, per molecule, at the graphite surface. Since the resistance of the adsorbed hydrocarbon films on graphite is not known, and since the contact resistance affects the efficiency of the performance of carbon brushes, a measurement of the graphite contact resistance under hydrocarbon atmospheres was included in the present project.

7.3 CURRENT PROGRESS

7.3.1 Literature Review of Lamellar Solids

The conventional solid brush for current collection is made of graphite or graphite-metal mixtures, and graphite is widely known as a solid lubricant with lamellar structure. In order to use up-to-date information on physico-chemical phenomena at solid surfaces to obtain an understanding of solid brush behavior, a comprehensive literature review has been made of the relevant chemical and physico-chemical properties of lamellar solids (mainly graphite and dichalcogenides of Mo, W, Nb and Ta and mixed dichalcogenides of these elements) and their interactions with metal surfaces.

7.3.1.1 Conclusions Drawn from the Literature Review

According to the published information, the following conclusions have been reached.

1. The lubricating properties of lamellar solids (graphite, dichalcogenides of Mo, W, Nb and Ta, mixed (quasibinary) dichalcogenides of $W_xNb_{1-x}Se_2$ types [where $x \sim 0.05$]), in terms of chemistry, are essentially governed by their crystal structure, the orientation and adhesion of their crystallites on the sliding surfaces, as well as their thermal and chemical stabilities under the sliding conditions. Modification of any of these properties directly affects the lubricating behavior of a solid brush.

2. Crystallites of lamellar solid lubricants are highly anisotropic in dimension and in physical properties. The peripheral

7-4

(edge) sites and dislocation cores at the prismatic (basal or the cleavage) planes are highly active, while the basal planes are of low surface energy. The edge-face interactions are important in disoriented powders or aggregates on the sliding surface, which lead to high friction and abrasive wear. Vapor lubrication, by introducing water vapor or vapors of hydrocarbons to the sliding system, prevents the reaggregation of the crystallites on sliding surfaces.

3. The transfer of lubricating film onto the metal (slipring) surface in air is very much dependent on the chemical nature of the metal substrate of the sliding system. Metal oxides present on the metal surfaces play a certain kind of role in the adhesion of the carbon films to the metal substrate, probably through C-O-metal bondings. Detailed information about the film transfer is incomplete at the present time. Adhesion of dichalcogenide lubricants on metal is stronger than that of carbon.

4. Surface oxides on metal rings also affect the wear rate of carbon brushes by catalytic oxidation when sliding in air. Oxides of lead, vanadium, manganese, and copper, which can be chemically reduced by carbon at elevated temperature to lower oxides or to the metallic state, lower the ignition temperature of graphite in air. More stable oxides, such as those of zinc, tungsten, tin, have little effect on graphite ignition temperature. In this respect, brass and bronze reduce the wear rate of graphite, but brass gives high voltage drops. Phosphorus bronze also lowers the friction of graphite. With regard to copper alloys, copper-zirconium alloys show the lowest friction to

graphite, as does phosphorus bronze, and the best quality (mechanical and thermal) among the presently available ring materials.

5. The wear phenomena of graphite in a solid brush are a combination effect of load, sliding speed, passage of current, and contact temperature. The contact temperature is more critical in the transition from adhesive wear to abrasive wear. Besides other physical and mechanical factors, increasing the critical transition temperatures by the use of additives, such as phosphorus-containing compounds to protect graphite crystallites from oxidation and disorientation, is important.

6. The thermal and chemical stabilities of solid lamellar lubricants are temperature dependent and vary with different ring metals in contact. These conclusions are useful guides for selection of materials for sliding systems and for the construction of self-lubricating solid brushes.

7.3.1.2 Recommendations from the Literature Review

The following recommendations were made for future work on solid brushes based on graphite and other lamellar solids. Details of work relevant to the present program are discussed in Section 7.3.3.

1. The use of straight-chain paraffinic hydrocarbons, to substitute for water vapor as additives to graphite in sliding contacts, needs to be fully investigated. Information on the temperature dependence of the stability of the adsorbed hydrocarbons on graphite is most necessary. Similar information for dichalcogenides would also be valuable.

2. In the investigation of vapor lubrication of graphite and dichalcogenides, brush samples made of powders of known properties of basal plane area are desirable for comparison of the lubrication effects.

3. The investigation of the mechanism of formation and transference of lubricating films is a basic approach to understanding the friction and wear behavior and also a guide for selection of slipring materials. This investigation should include not only the effect of composition and surface treatment of the sliding materials but also the effect of the presence of various vapors.

4. The use of phosphorus compounds such as $(NH_4)_2HPO_4$ and $POCl_3$ as antiwear additives for graphite needs to be fully investigated. Impregnation techniques and their effects on frictional loss and resistive loss should also be emphasized.

5. Synthesis and evaluation of quasibinary dichalcogenides of $W_xNb_{1-x}Se_2$ and $Mo_xTa_{1-x}Se_2$ types (where $x \simeq 0.05$) need to be initiated. The crystal structure and electrical conductivity and their relation to composition of the quasibinary compound are the main items to be concerned with. Evaluation of the dichalcogenides should include the effects of various environmental conditions.

7.3.2 Contact Phenomena

The contact resistance of graphite under vacuum and under several paraffinic hydrocarbon vapor atmospheres was measured by a crossed-rod technique. Two kinds of graphite (electrographite W417 from Stackpole Carbon, density $\sim 1.6 \times 10^3$ kg/m^3, and SPK from National Carbon Company,

apparent density $\sim 1.9 \times 10^3$ kg/m^3) were selected for the measurements. Four hydrocarbons (n-heptane, n-decane, n-dodecane, and n-hexadecane, all commercial products of high purity) were used, separately, as the vapor source.

7.3.2.1 Experimental

The crossed-rod system used in this work is very similar to the system described by Went and the complete system is depicted schematically in Figure 7.1. The crossed-rod system was enclosed in a Pyrex glass tube (3.8 cm diameter). The rods of graphite (0.3175 cm diameter and 3.175 cm long) were separately and tightly connected to nickel wires by means of copper clamps at the ends of the rods. The lower rod was also fixed in position by the copper clamps to a solid copper ring which rested on the ring portion of the glass tube to prevent the rod from moving. The nickel wires of the upper rod were welded on two small springs. Since the springs and the nickel wires of the lower rod were connected to the four leads sealed in the glass wall, the upper rod could be suspended free above, and at right angles to, the lower rod in the Pyrex tube. By means of a nickel wire hook, the weight (an iron slug of ~ 15 g) could pull the upper rod down, leaving a gap of ~ 0.5 mm to the lower rod. The weight could be further pulled down by a solenoid mounted underneath the glass tube. As the current in the solenoid, monitored by a calibrated variable resistance, was increased, the upper rod was brought into contact with the fixed rod. The contact load could then be applied by further increasing the

current in the solenoid. The four terminal leads outside of the glass tube were connected to a portable precision Kelvin bridge for contact resistance measurement. The contact resistances were first measured under vacuum at contact loads up to 10.0 g. Each measurement was started with a new contact-make. Hydrocarbon vapors were then introduced into the system on test at a controlled rate by the variable leak valve and the contact resistance measurements were then repeatedly carried out under the same vapor at different pressures. Vapor pressure of the hydrocarbon at different levels were monitored by a magnetic-ion-pump control unit, an ionization gauge, and a thermocouple gauge.

7.3.2.2 Results and Discussion

A total of five series of contact resistance measurements was carried out with five pairs of graphite rods. The contact resistance data for each series, obtained under vacuum, and under different pressures of hydrocarbon vapors, are plotted against contact loads on a log-log scale in Figures 7.2-7.4.

The variation of contact resistance with load has a power-law behavior. These data also show that the electrical resistance of the graphite contacts increased in the presence of admitted hydrocarbon vapors and with increasing vapor pressures. The slopes of these straight lines are about -1/2 (Figures 7.3 and 7.4) and somewhat higher than -1/2 (Figure 7.2). In the case of clean, smooth metal surfaces, these slopes would imply that the contact surface was generated by purely plastic deformation. Due to the porous nature of the graphite

7-9

rods, the contact area in this case may not have been circular, but may have consisted of several discrete contact spots. Increasing load would have caused the size of these contact spots to increase, but at the same time, new small spots may have been created, causing the apparent contact resistance to be lower at higher loads. Throughout these measurements, the contact loads were limited to the range of 2.0 to 9.0 g, which are small, and we can only assume that the contact area was produced by elastic deformation.

The film resistance of the adsorbed hydrocarbons on graphite can be derived from these measurements by subtracting the contact resistance under vacuum from the contact resistance observed under hydrocarbon vapors at the corresponding load. The numerical value of contact resistance may be taken from the normalized straight lines in Figures 7.2-7.4. The resulting film resistance is summarized as a function of hydrocarbon pressures in Table 7.1.

From Table 7.1, it can be seen that, for a specific pair of graphite rods, the film resistance varied with load and increased with increasing vapor pressure of hydrocarbon in the contact surroundings. For graphite W417 rods under contact load of 4.0 g, for example, the film resistance was calculated to be 0.06 to 0.11 Ω under vapor pressure of 1.33 x 10^{-3} N/m^2, 0.15 to 0.16Ω under 2.66 x 10^{-2} N/m^2, and 0.19 to 0.21 Ω under 0.88 N/m^2. The film resistance appeared to be the same magnitude within a factor of 2 under the same pressure and contact load for all the hydrocarbons (n-heptane, n-decane, and n-dodecane) of interest, regardless of their carbon-chain length. The same conclusion

7-10

also applied to the film resistance with the graphite SPK rods. The results imply that the voltage drop of sliding electric contacts in a current collector would be the same when all n-paraffinic hydrocarbons are used as vapor additives.

N-paraffinic hydrocarbon molecules are thought to be adsorbed on the basal planes of graphite surfaces in an orientation such that the hydrogen atoms, which are closest to the graphite surface, lie at the centers of carbon hexagons of the graphite basal planes. Similar flat orientation of adsorbed n-paraffinic hydrocarbons (from n-hexane to n-hexadecane) on clean polished surfaces of metals was also concluded from surface potential measurements. When the hydrocarbon molecules adsorb horizontally on a graphite surface and are oriented with a maximum number of atoms (hydrogen) contacting the surface, only the cross-section of the molecule contributes to the film resistance in the resistance measurements. Since the cross-section ($-CH_2-$) is the same for all n-paraffinic hydrocarbons in orientated configurations, the film resistance might be expected to be similar, as observed here.

7.3.3 New Concepts for Development

Several new concepts for brush development are described in this Section. Also included are those research areas and problems which are not directly involved in the brush development but which are directly related to the contact system and for which continuing efforts are required in the future.

7.3.3.1 Metal Plated Carbon Fiber Brushes

These have been shown to be capable of transferring fairly high currents (up to 1.55 MA/m^2) in continuous operation and operating at speeds up to 100 m/s with moderate electrical and frictional losses. The basic form of the brush is one in which carbon fibers are coated with some metal, preferably one offering low electrical (and frictional) losses. Conduction takes place primarily through this coating, with the fiber providing mechanical strength and, possibly, some lubrication. Several different coatings have been employed, and effort has been expended at Westinghouse (see Section 6.3) as well as elsewhere, to develop coating techniques.

At present, we have the capability for plating relatively short lengths of this material, primarily with silver, although other coatings are possible.

Present effort is devoted to making a number of small brushes for experimental tests with a view of optimizing brush design. In particular, it is intended that the benefits arising from the potentially excellent internal heat transfer capabilities of the multifiber brush should be characterized. Single fiber tests have shown that in a natural convection mode of coating, current densities in the metallic fiber coating in excess of 12 GA/m^2 can be transmitted without the fiber being destroyed. While it is not anticipated that similar levels can be achieved in a multifiber brush, considerable improvement over present brush cooling techniques appears possible.

7.3.3.2   Brushes Made of Oleophilic Graphite

Oleophilic graphite is produced by grinding graphite under a
liquid hydrocarbon. In this way, the ratio of surface-to-edge sites is
appreciably modified compared to ordinary graphite, with over 99% of the
material being in the form of thin (< 50 Å), but large, basal planes.
The resulting material may be used either in the form of a gel in a
hydrocarbon liquid or as a solid. In the latter case, metal-graphite
mixtures can be produced in which the metal content is up to 95%. The
resulting compressed compacts are said to be very stable (because the
chemistry of the edge sites is modified) and have better lubricating
ability than MoS_2.

7.3.3.3 Concepts for Long-Term Research

In the longer term, it is planned that the following approaches
will be investigated: (1) phosphorous compound impregnation, (2) dichalco-
genides, (3) solid hydrocarbon additives, and (4) intercalated graphites.

7.3.3.3.1 Phosphorus Compounds Impregnation

Phosphorus-containing compounds, including phosphates of
aluminum, zinc, copper, phosphoric acid, and phosphorus oxyhalides, have
been known as effective oxidation inhibitors for graphite since the use
of graphite as a moderator in nuclear reactors. Recent work done at

General Electric indicated that, in the presence of ammonium phosphates or phosphorus oxyhalides, the ignition temperature of graphite in air was increased significantly. The addition of small amounts of these phosphorus compounds into a carbon brush has, therefore, been suggested for lowering the wear rate of the brush in electric contacts. Some experimental work on wear and friction measurements has been reported by Lancaster, but no data on voltage drops in brush contacts have been published.

Although the exact mechanism by which these additives affect friction and wear is not yet fully understood, an investigation into additives of this type seems worthwhile for carbon brushes which have to be used in high speed and/or high current machines, where contact temperatures will be high, and conventional brushes wear away rapidly by oxidative processes.

Phosphates of ammonium (monobasic and dibasic) and phosphorus oxychloride appear to be more suitable as additives for carbon brushes than other phosphorus-containing compounds. Ammonium phosphates thermally decompose to ammonia and phosphorus pentoxide, and only the latter will actively remain on the carbon brush. Phosphorus oxychloride is a liquid, excess amounts of which will be evaporated away at elevated temperature, but the adsorbed phosphorus oxychloride is reported to be stable up to 400°C.

Experimental work in this area should include: impregnation methods; the evaluation of the impregnated brushes (friction, wear, voltage drop) at high speeds and current densities; and optimization of the impregnation levels.

7-14

7.3.3.3.2 Dichalcogenides

Dichalcogenides (mainly disulfides and diselenides) of W, Mo, Nb, and Ta are solid lubricants with lamellar crystal structures. Unlike graphite, the antifriction properties of the dichalcogenides are generally good under vacuum but poor in air. The friction coefficients of all the dichalcogenides except WSe_2, increase with increasing humidity of the air. $NbSe_2$ and $TaSe_2$ exhibit metallic conductivity while others are poor conductors. Indications from several Russian papers have been that the quasi-binary systems of the $Nb_xW_{1-x}Se_2$ and $Ta_xMo_{1-x}Se_2$ type (where $x \sim 0.05$), have a combination of good electrical, and antifriction properties both in vacuum and in air of high humidity. Materials of this type have, therefore, been suggested as promising candidates for electrical contact applications. The remaining outstanding problem is the synthesis of such materials with the correct crystal structure, mainly because stacking defects in the layers, which affect the crystal lattice parameters and also the antifriction behavior, arise during crystallization of these compounds.

A program for the development of these kinds of materials should include: preparation of stoichiometric diselenides of W, Mo, Nb, and Ta by capsule technique and by interaction of metal oxides and H_2Se, the effect of annealing conditions on the stoichiometry of the resulting compound; preparation of $Nb_xW_{1-x}Se_2$ by capsule technique with elements, Nb-W alloys and selenium, and mixtures of $NbSe_2$ and WSe_2; study of the effect of annealing conditions to the stacking errors of the final crystals; study of recrystallization process for eliminating the stacking defects

from the final crystals; and evaluation of the electrical and antifriction properties of the products. Similar steps can be applied to the development of $Ta_xMo_{1-x}Se_2$ materials. Where possible, commercially available materials should also be purchased and characterized experimentally.

7.3.3.3.3 Hydrocarbon Additives

The lubricating properties of graphite are well known to be dependent upon the presence of water vapor in the atmosphere. Under vacuum, graphite wears away rapidly upon sliding, but severe wear can be prevented by introducing small quantities of vapors of n-paraffinic hydrocarbons, alcohols, or halides into the sliding environment. These early findings, from General Electric, were called vapor lubrication. Recent studies of selective adsorption on graphite and molybdenum disulfide at the British Petroleum Research Center indicate that these lamellar solids have specific affinity to adsorb long-chain molecules of hydrocarbons on their crystal basal planes. We have applied several long-chain hydrocarbons (from n-heptane to n-hexadecane) as vapor additives for carbon brushes for lowering the wear rate. Preliminary results (see Section 5.3.2) showed that, in carbon dioxide atmospheres, the brush life can be extended by a factor of 3 in the presence of these vapors.

The use of hydrocarbons as a vapor additive and as a substitute for water vapor in sliding systems has several advantages: (1) for lowering the wear rate, the minimum vapor pressure (in the range of 10 to

less than 1 N/m^2) is much less than that of water vapor (minimum 400 N/m^2), this leads to easy control of the vapor concentration in the atmosphere; (2) unlike water, the effective vapor pressure of hydrocarbon is far below its saturated vapor pressure so that no condensation should occur in the sliding system.

Further work on the use of hydrocarbon vapor additives should include: (1) evaluation of n-paraffinic hydrocarbons higher than hexadecane (those solid hydrocarbons can be directly added to carbon brush by impregnation); (2) evaluation of cyclic hydrocarbons, including benzene, naphthalene, and others; (3) evaluation of the pressure dependence on the frictional behavior of carbon brush for the most efficient hydrocarbons; and (4) evaluation of the temperature dependence of the frictional behavior of carbon brushes at several different vapor pressures of the most efficient hydrocarbons.

7.3.3.3.4 Intercalated Graphites

The structure of graphite can be significantly modified, and indeed new compounds formed, by reaction with other materials. Special cases are the intercalants, in which appreciable interest has recently been shown. Intercalants fall into two main groups, generally classified (by analogy with semi-conductors) as donor and acceptor materials. The donor materials (alkali metals) are extremely unstable, mostly in air but, in some cases, even in nitrogen. The acceptor materials (generally acids) are more stable and have a higher electrical conductivity. The structure produced by intercalating the graphite is essentially that of

a two-dimensional metal so that the conductivity, and other properties, are highly anisotropic.

During the last two years, considerable interest in acceptor intercalated graphite has been aroused by the claim that conductivities higher than copper could be achieved by the use of antimony pentafluoride as an intercalant. Although more recent work does not appear to have full substantiated earlier claims, there is still a good chance that this new range of materials could produce fruitful areas for brush development, especially since the essentially two-dimensional planar structure probably implies a low friction coefficient, although this has not been investigated.

In addition to solid graphite, fibers can be intercalated (with nitric acid, for example), and it is known that this produces an increase in their conductivity by an order of magnitude or more. The dichalcogenides (see Section 7.3.2.2.2) may also be intercalated.

A program to investigate these materials with a view to ascertaining their suitability for brushes would seem to be very worthwhile.

7.3.3.4 Continuing Research Areas and Problems

Besides those new concepts for near-term and longer-term research targets, a continuing effort should be employed on: (1) slipring material development, (2) atmosphere control (including additives), (3) temperature control, and (4) fundamental interface investigations.

7.3.3.4.1 Slipring Material Developments

The basic properties (hardness, thermal and electrical conductivities, thermal strength, and chemical stabilities) of slipring material directly affect the lubricating behavior of a solid brush. The operational parameters of silver and noble metal sliprings and brushes have been extensively studied for space application. However, less work has been done for copper and copper alloys operating under normal conditions. This limited information has shown that in copper alloys, the phosphorus bronzes (containing less than 10% Sn), some copper-nickel alloys (the Monels), and copper-zirconium alloys reduce the friction coefficient of carbon brushes. Detailed effects on alloy composition and correlation to the basic properties of the alloys are not known.

Further developments of slipring materials should include two categories. (1) For copper alloys (Cu-Sn, Cu-Ni, Cr-Zr, and others) the operational parameters (friction, wear, and voltage drop) should be studied as a function of alloy composition. Physical properties of the alloys should be recorded for comparison with the operational parameters. (2) For double- or multi-layered ring materials, including copper-faced steel, noble metal (rhodium or gold and rhodium)-plated copper or steel, and others, the operational parameters should be studied with products obtained from different techniques (powder metallurgy, electrochemical plating, and metal spraying). Recent evidence from high speed tests at the University of Texas apparently shows a substantial difference between electrical performance (brush voltage drop) of electroplated and flame-sprayed copper on steel.

7-19

7.3.3.4.2 Atmosphere Control

Experiments in atmospheres other than air have clearly shown that brush performance is dependent on the nature, temperature, and pressure of the surrounding gas. For example, Pardee showed that the quantity of water vapor required to prevent dusting was dependent on the gas in which the water vapor was suspended. Experiments by Savage and others (recently extended here) have shown that vapors other than water can also be beneficial in some aspects of brush behavior. For example, by lowering friction and wear, although possibly at the expense of an increased voltage drop.

It is apparent that the molecular properties of the slipring-brush-film-gas-vapor interface play an important part in determining the properties of the physi- or chemi-sorbed films which, in turn, are responsible for the observed frictional, electrical, and wear characteristics of the sliding contact.

To a large extent, this explains why, despite the many years of practical experience, this field remains highly empirical. However, modern diagnostic aids are available which, when used in parallel with experimental screening tests, should enable some advances to be made in understanding why particular atmospheres are beneficial under defined brush operating conditions.

7.3.3.4.3 Temperature Control

Experimental investigations have shown that the dusting phenomenon is strongly dependent on the temperature of brush operation. Although not yet fully proven, it is likely that this arises from the desorption of adsorbed water vapor in the temperature range 140 to 200°C. Provided the bulk brush interface temperature can be kept below this range, satisfactory (i.e., non-dusting) operation can apparently be assured, even though the individual contact spot temperatures may transiently exceed these levels.

It, therefore, seems likely that brush operating reliability could be significantly improved if brush and slipring temperature control could be improved to assure that these critical temperatures are not exceeded. Methods of improving temperature control need to be assessed and experimentally verified. Possible techniques for cooling brushes and rotors include external gas, liquid and evaporative cooling, internal cooling, and the use of heat pipe techniques.

7.3.3.4.4 Fundamental Interface Investigations

Study of the formation and the composition characteristics of the lubricating films in a sliding contact system under different environments, is a fundamental approach to provide basic information about the influence of materials and environments on the characteristics of friction and wear. Some work has been done at NASA Lewis Research Center in Cleveland, Ohio, mainly on metal-metal systems for space programs. Only two short notes (which appeared recently in Russian

7-21

journals) deal with graphite-copper systems in air.   Information on the graphite-metal systems under defined conditions is urgently needed to aid the understanding of the interactions at electric contacts and also as a guide for the selection of contact members and contact conditions. Two systems for studying the formation and physical and chemical characteristics of the lubricating films, consisting of sliding test-rigs enclosed in a high vacuum system, have been considered by the authors. The surface conditions (surface finishing and oxidation state) of the contact members will be controlled for these studies. One system with low sliding speed could be fitted to the stage of an Auger spectrometer so that the formation and chemical composition of the lubricating film can be observed directly during sliding. This would yield invaluable, and hitherto unobtainable, information on the films generated in sliding electrical contacts. The other system with controlled sliding speeds could be used for studying the physical and chemical natures of the lubricating films obtained after operation under controlled conditions. Analytical techniques for investigation of the films will include x-ray diffraction (for grain size and phase structures), scanning electron microscopy (film thickness and structure), and x-ray microprobe analysis (chemical composition). Friction coefficients, wear rates, and voltage drops can be obtained by conventional methods during the experiment.

Efforts should also be devoted to exploring the effects of surface oxide on metals or alloys on the transfer of carbon-containing lubricating films and the lubricating properties of graphite or graphite

containing solid brushes, the effects of atmosphere (humidity and vapor additive) on the film characteristics, and the combination effect of the metal surface and the atmosphere on the film characteristics.

TABLE 7.1

SUMMARY OF ELECTRICAL RESISTANCE OF HYDROCARBON FILMS ON GRAPHITE

Partial Pressure of Hydrocarbon, N/m^2

Film Resistance, Ohm

| Load, g Hydrocarbon/Graphite	1.33×10^{-3}				2.66×10^{-2}				0.88			8.8		
	2.0	3.0	4.0	6.0	2.0	3.0	4.0	6.0	2.0	4.0	6.0	3.0	4.0	6.0
n-Heptane/SPK	0.3	0.24	0.19	0.15	0.52	0.42	0.34	0.27				0.86	0.75	0.61
n-Hexadecane/SPK (10^{-4} N/m^2)	0.37		0.27	0.20										
n-Heptane/W417		0.12	0.08			0.22	0.16	0.09		0.19	0.16 (load 5g)			
n-Decane/W417	0.17		0.11	0.09	0.59		0.44	0.37						
n-Dodecane/W417	0.06		0.06	0.06	0.21		0.15	0.13	0.25	0.21	0.20			
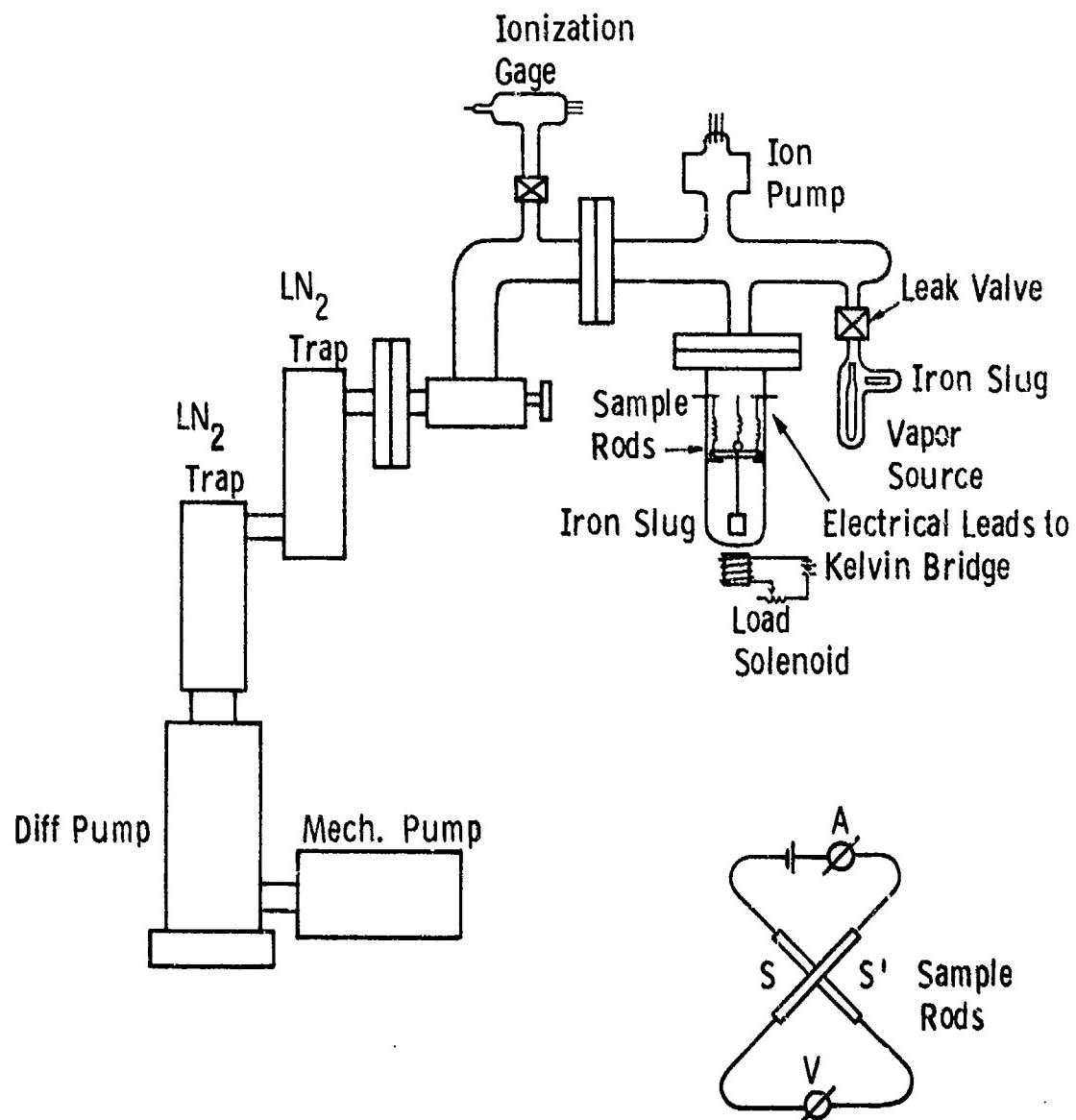
Figure 7.1: Schematic Diagram of Contact-Resistance Measurement System

(B) Contact Resistance of Graphite (SPK)
1. Under Vacuum
2. Under n-hexadecane vapor,
6.7×10^{-4} N/m^2

Contact Load, g

(A) Contact Resistance of Graphite (SPK)
1. Under Vacuum
2. Under n-heptane vapor, 1.33×10^{-3} N/m^2
3. Under n-heptane vapor, 2.66×10^{-2} N/m^2
4. Under n-heptane vapor, 8.8 N/m^2

Contact Load, g

Contact Resistance, ohm
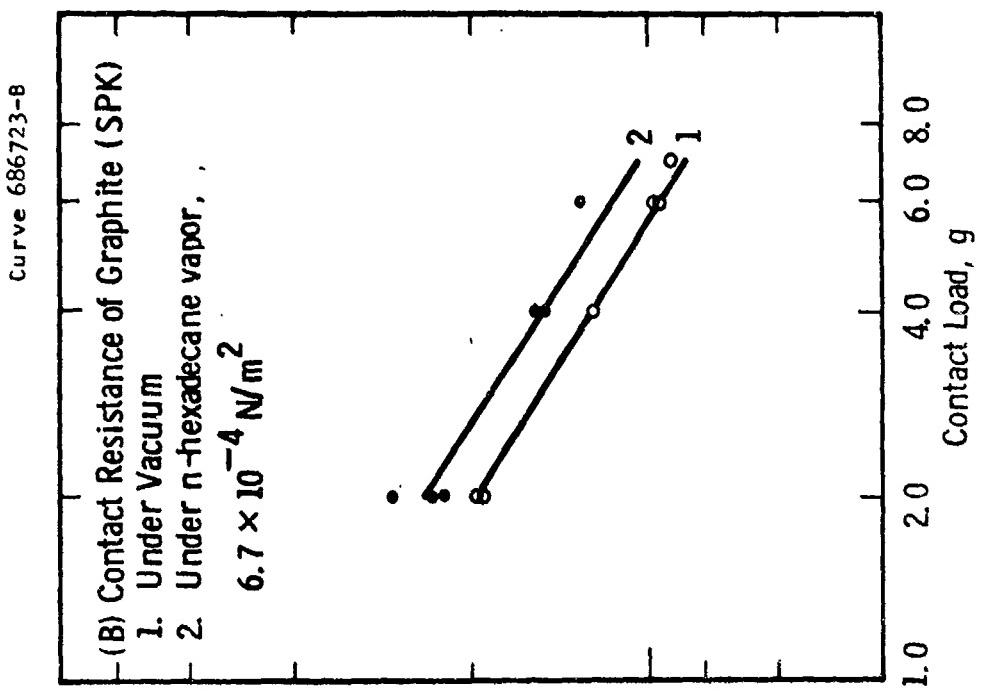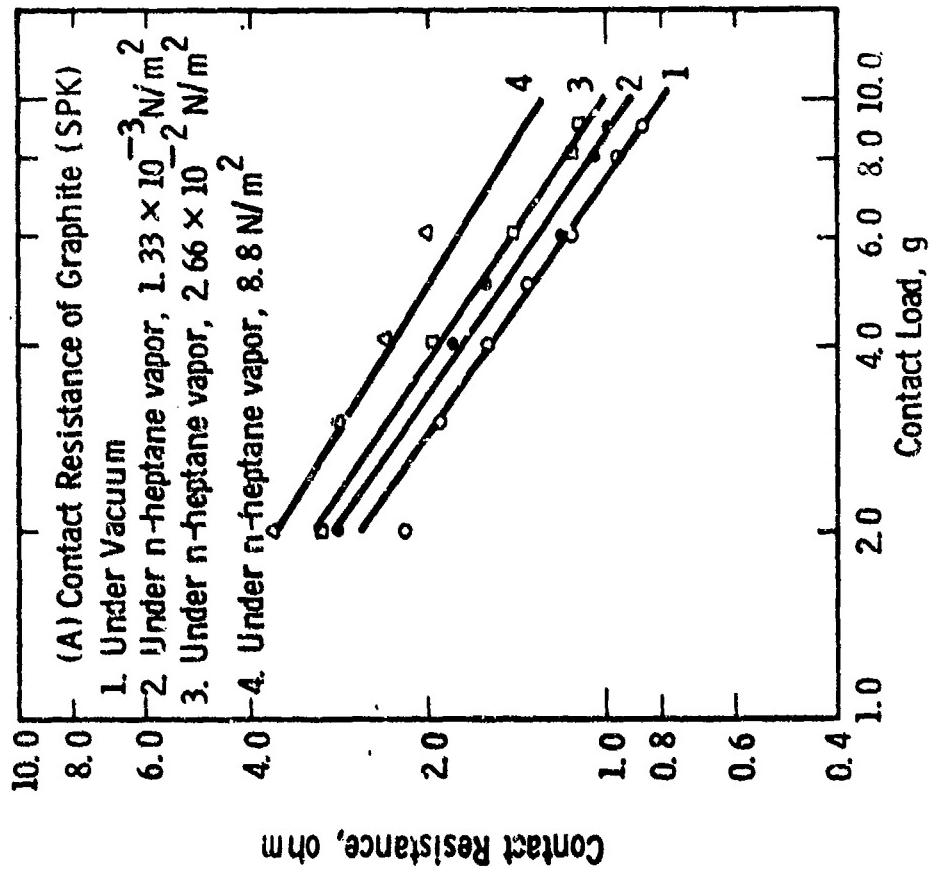
Figure 7.2: Contact Resistance of Graphite vs. Load Under Vacuum, Under
n-heptane vapor (A) and under n-hexadecane vapor (B).
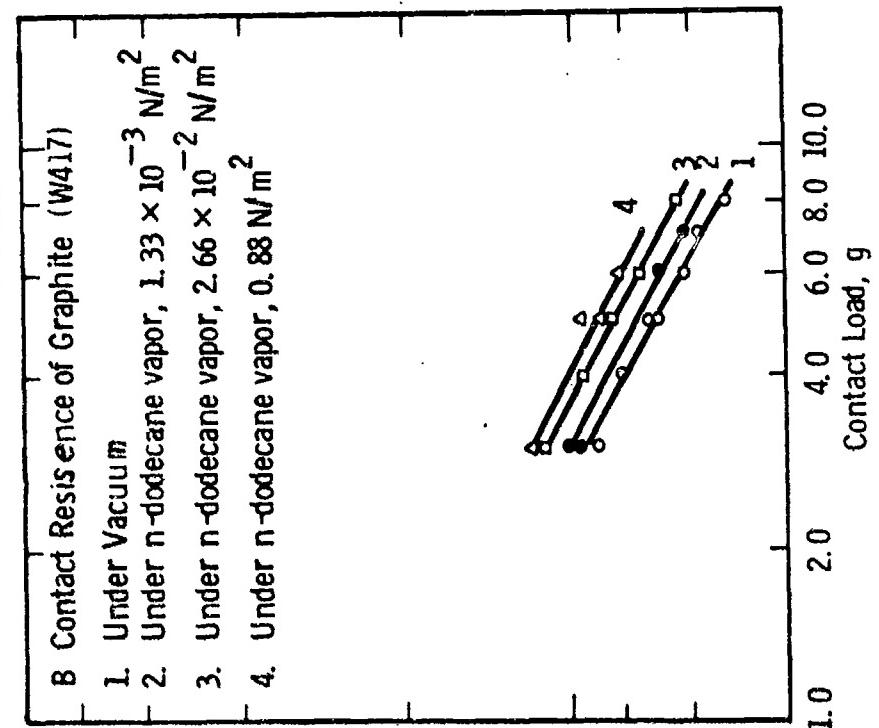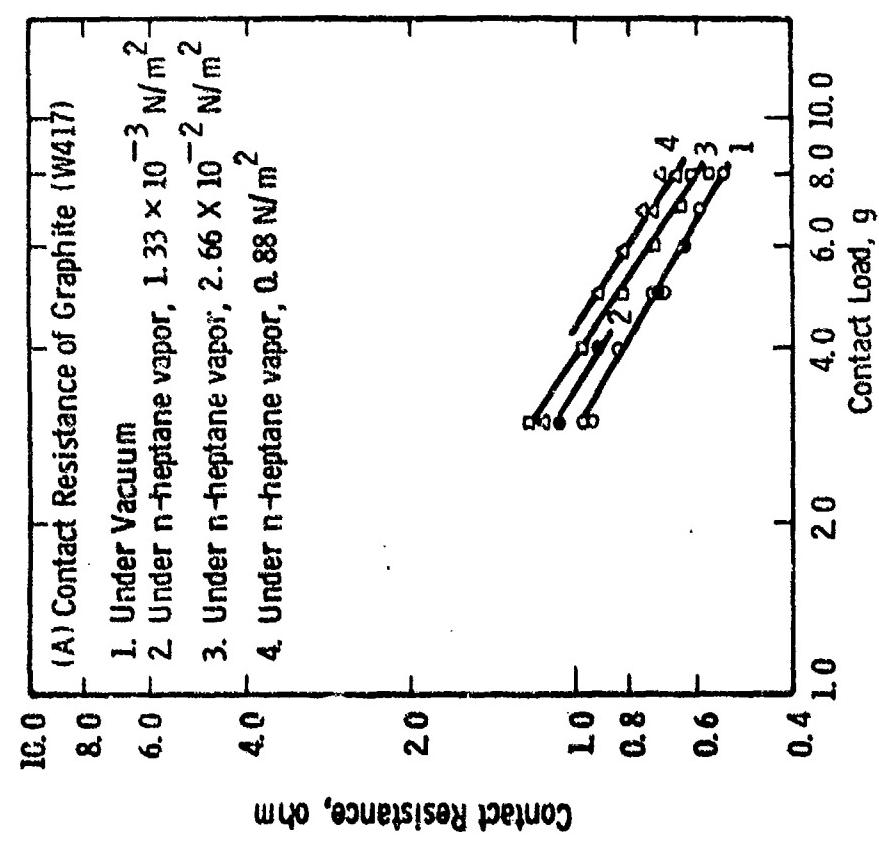
Figure 7.3: Contact Resistance of Graphite vs. Load Under Vacuum, Under n-heptane vapor (A) and under n-dodecane vapor (B).
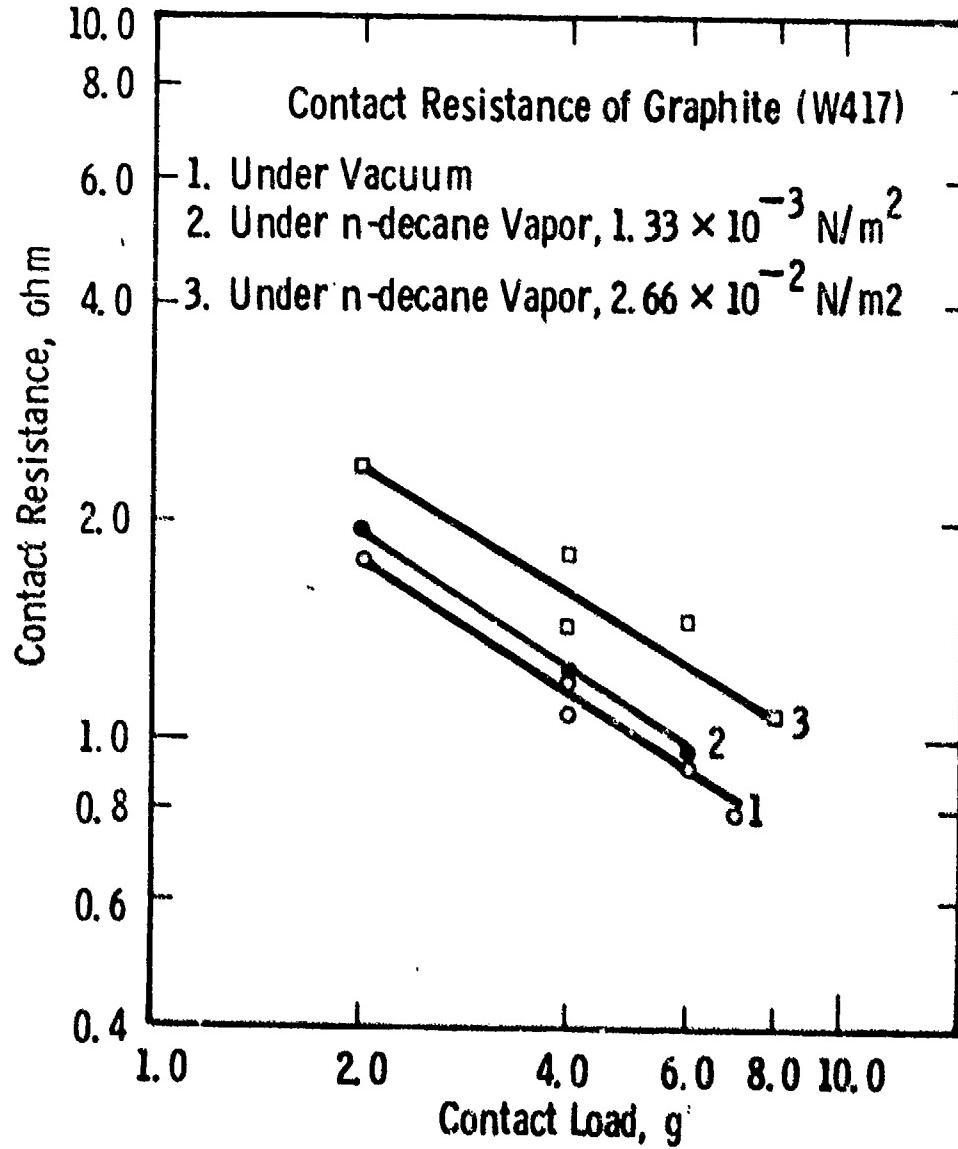
Figure 7.4: Contact Resistance of Graphite vs. Load Under Vacuum and Under n-decane Vapor.